

# A theory vade mecum for PSI experiments

G. Colangelo<sup>1</sup>, F. Hagelstein<sup>2</sup>, A. Signer<sup>2\*</sup>, and P. Stoffer<sup>3</sup>

<sup>1</sup> Albert Einstein Center for Fundamental Physics, Institute for Theoretical Physics,  
University of Bern, Switzerland

<sup>2</sup> Paul Scherrer Institut, 5232 Villigen PSI, Switzerland

<sup>3</sup> University of Vienna, Faculty of Physics, Boltzmannngasse 5, 1090 Vienna, Austria

\* adrian.signer@psi.ch

May 17, 2021



*Review of Particle Physics at PSI*  
doi:[10.21468/SciPostPhysProc.2](https://doi.org/10.21468/SciPostPhysProc.2)

## Abstract

This article gives a compact introduction and overview of the theory underlying the experiments described in the rest of this review.

## 5.1 Introduction

The purpose of this article is to give a broad overview of the theory background to the experiments that have been and are carried out at the Paul Scherrer Institute. Space limitations make it impossible to go into depth or provide a self-contained theoretical summary. Much more modestly, we aim to put the experiments into context and provide key references for further reading. The experiments we refer to are listed in Table 5.1 and they will be described in greater detail in separate sections/articles of the Review of Particle Physics at PSI [1–23]. From a theory point of view, these experiments either lead to precise determinations of physical parameters required as input for other experiments, test the interactions of the Standard Model (SM), or search for and constrain physics beyond the Standard Model (BSM). In the following we aim to give meaning to these three statements.

After a general overview of the theoretical methods applied to describe the processes and bound states in Table 5.1, we will, in turn, consider the muon, the proton, nucleons and nuclei, the free neutron, and the pions.

## 5.2 Overview

The experiments we are primarily concerned with involve low-energy interactions of electrons, muons, protons, neutrons, and pions. Their dynamics is described by the SM, the gauge theory of strong and electroweak interactions. In view of the large masses of the Higgs and weak gauge bosons, the weak part of the SM Lagrangian is essentially frozen at low energies (it will later be considered as a small correction). In this regime, the SM reduces to the standard QED and QCD Lagrangian

$$\mathcal{L}_{\text{QED+QCD}} = \sum_f \bar{f} (i\not{D} - m_f) f - \frac{1}{4} F_{\alpha\beta} F^{\alpha\beta} - \frac{1}{4} G_{\alpha\beta} G^{\alpha\beta}, \quad (5.1)$$

where the electromagnetic and gluonic field-strength tensors are expressed in terms of the photon and gluon fields,  $A^\alpha$  and  $G^\alpha$ , as  $F^{\alpha\beta} = \partial^\alpha A^\beta - \partial^\beta A^\alpha$ ,  $G^{\alpha\beta} = \partial^\alpha G^\beta - \partial^\beta G^\alpha - ig_s [G^\alpha, G^\beta]$ , and where for clarity we have omitted gauge-fixing and ghost terms. The sum runs over all

experiment	section	process / particles / (bound states)
[1] muon decay	6	$\mu^+ \rightarrow e^+ \nu_e \bar{\nu}_\mu$
[2] MuLan	16	$\mu^+ \rightarrow e^+ \nu_e \bar{\nu}_\mu$
[3] Sindrum	7	$\mu^+ \rightarrow e^+ ee, \mu^+ \rightarrow e^+ \nu_e \bar{\nu}_\mu ee, \pi^+ \rightarrow e^+ \nu_e ee, \pi^0 \rightarrow ee$
[4] Sindrum II	8	$\mu^- \frac{A}{Z}N \rightarrow e^- \frac{A}{Z}N$ for Au, Pb, Ti
[5] MEG	19	$\mu^+ \rightarrow e^+ \gamma, \mu^+ \rightarrow e^+ \nu_e \bar{\nu}_\mu \gamma, \mu^+ \rightarrow e^+ X \rightarrow e^+ \gamma \gamma$
[6] Mu3e	20	$\mu^+ \rightarrow e^+ ee, \mu^+ \rightarrow e^+ \nu_e \bar{\nu}_\mu ee$
[7] Mspec, Mu-Mass	29	$M = (\mu^+ e^-), \mu^+$
[8] MACS	9	$M = (\mu^+ e^-) \leftrightarrow \bar{M} = (\mu^- e^+)$
[9] CREMA	21	$(\mu^- p), (\mu^- d), (\mu^- \text{He}), p, d, \text{He}$
[10] muX	22	$(\mu^- \frac{A}{Z}N), {}^{248}_{96}\text{Cm}, {}^{226}_{88}\text{Ra}$
[11] MUSE	23	$e^\pm p \rightarrow e^\pm p, \mu^\pm p \rightarrow \mu^\pm p$
[12] MuCap	17	$\mu^- p \rightarrow \nu_\mu n$
[13] MuSun	18	$\mu^- d \rightarrow \nu_\mu nn$
[14] pionic deuterium	14	$(\pi^- p), (\pi^- d)$
[15] pionic helium	26	$(\pi^- e^- {}^4\text{He}^{++}), \pi^-$
[16] nTRV	15	$n \rightarrow pe^- \bar{\nu}_e$
[17] nEDM	27	$n, n$
[18] nEDMX	28	$n$ / dark matter / exotic
[19] negative pions	10	$(\pi^- p), \pi^-$
[20] positive pions	11	$\pi^+ \rightarrow \mu^+ \nu_\mu, \pi^+, \nu_\mu$
[21] neutral pions	12	$\pi^- p \rightarrow \pi^0 n, \pi^0$
[22] PiBeta	24	$\pi^+ \rightarrow \pi^0 e^+ \nu_e, \pi^+ \rightarrow e^+ \nu_e (+\gamma), \mu^+ \rightarrow e^+ \nu_e \bar{\nu}_\mu \gamma$
[23] PEN	25	$\pi^+ \rightarrow e^+ \nu_e (+\gamma), \mu^+ \rightarrow e^+ \nu_e \bar{\nu}_\mu \gamma$

Table 5.1: Processes and particles (bound states) that are investigated at PSI, where the driving interaction to be studied is indicated by the color as follows: **BSM**, **weak**, **weak and try to learn about strong**, **EM**, **EM and try to learn about strong**, **strong**. In addition the mass or charge radius of particles are measured. The section number refers to the Review of Particle Physics at PSI.

37 fermions of mass  $m_f$ , electric charge  $eQ_f$ , and color charge  $g_s t_f^a$ , and the covariant derivative  
 38 acts on the fermion fields as  $D_\alpha f = (\partial_\alpha - ieQ_f A_\alpha - ig_s t_f^a G_\alpha^a) f$ . For  $f = \ell \in \{e, \mu, \tau\}$  we have  
 39  $Q_\ell = -1$  and  $t_\ell^a = 0$ , whereas for quarks  $Q_u = 2/3$ ,  $Q_d = -1/3$ , and  $t_{u,d}^a = \lambda^a/2$  with Gell-  
 40 Mann matrices  $\lambda^a$ . In several experiments of interest here the photon acts as a probe: it is  
 41 coupled to the electromagnetic current  $J_{\text{em}}^\alpha$  as

$$\mathcal{L}_{\text{QED}}^{\text{int}} = e A_\alpha J_{\text{em}}^\alpha \equiv e A_\alpha \sum_f Q_f \bar{f} \gamma^\alpha f. \quad (5.2)$$

42 If we use (5.1) to compute the matrix element of  $J_{\text{em}}^\alpha$  between two states of pointlike leptons  
 43  $\ell$  with momenta  $p_1$  and  $p_2 = p_1 + q$ , we find

$$\langle \ell(p_2) | J_{\text{em}}^\alpha | \ell(p_1) \rangle = \bar{u}(p_2, m_\ell) \left( F_1^{(\ell)}(q^2) \gamma^\alpha + F_2^{(\ell)}(q^2) \frac{i \sigma^{\alpha\beta} q_\beta}{2m_\ell} \right) u(p_1, m_\ell), \quad (5.3)$$

44 where  $u$  and  $\bar{u}$  are the usual spinors. The decomposition (5.3) directly follows from the Lorentz  
 45 and  $U(1)_{\text{em}}$  gauge symmetries of the theory and is valid beyond perturbation theory. While  
 46  $F_1^{(\ell)}$  is related to the electric charge,  $F_2^{(\ell)}$  is related to the anomalous magnetic moment (AMM)  
 47 of  $\ell$  as

$$F_2^{(\ell)}(0) = a_\ell = \frac{(g-2)_\ell}{2}. \quad (5.4)$$

48 In contrast to the leptons, quarks do not appear as free particles in nature, but are confined  
 49 inside hadrons by the strong interaction. The general principles on which the decomposi-  
 50 tion (5.3) is based, also hold for non-pointlike particles, such as the nucleons  $N \in \{p, n\}$

$$\langle N(p_2) | J_{\text{em}}^\alpha | N(p_1) \rangle = \bar{u}(p_2, m_N) \left( F_1^{(N)}(Q^2) \gamma^\alpha + F_2^{(N)}(Q^2) \frac{i \sigma^{\alpha\beta} q_\beta}{2m_N} \right) u(p_1, m_N), \quad (5.5)$$

51 where we have introduced the common definition  $Q^2 \equiv -q^2$ . A relation between the AMM  
 52 and  $F_2^{(N)}$  analogous to (5.4) still holds. However, this quantity depends on strong dynamics,  
 53 which at low energies cannot be computed in perturbation theory.

54 In the case of the nucleons, often the electric and magnetic form factors

$$G_E^{(N)}(Q^2) \equiv F_1^{(N)}(Q^2) - \frac{Q^2}{4m_N^2} F_2^{(N)}(Q^2), \quad G_M^{(N)}(Q^2) \equiv F_1^{(N)}(Q^2) + F_2^{(N)}(Q^2) \quad (5.6)$$

55 are used. In the limit of small  $Q^2$  all form factors  $F_i(Q^2)$  can be understood as the Fourier trans-  
 56 form of an extended classical ‘charge’ distribution  $\rho_i(r)$  in the Breit frame where  $q^\mu = (0, \vec{q})$ .  
 57 Upon expansion in small  $Q^2$  we get

$$F_i(Q^2) = \int d^3\vec{r} e^{-i\vec{q}\cdot\vec{r}} \rho_i(r) = \int d^3\vec{r} \rho_i(r) - \frac{1}{6} Q^2 \int d^3\vec{r} r^2 \rho_i(r) + \dots \quad (5.7)$$

58 This leads to a general expression for the second moment of the charge distribution  $\rho_i$

$$r_i^2 \equiv \frac{1}{N} \int d^3\vec{r} r^2 \rho_i(r) = -6 \frac{1}{N} \left. \frac{dF_i(Q^2)}{dQ^2} \right|_{Q^2=0}, \quad N = \begin{cases} 1 & \text{if } F_i(0) = 0, \\ F_i(0) & \text{else.} \end{cases} \quad (5.8)$$

59 The relation above is used for example to determine the root-mean-square,  $R_i = \sqrt{r_i^2}$ , charge  
 60 and magnetic radii of the proton as well as the axial radius of the nucleon.

61 If we now consider the weak interactions, we must arrange fermions into left-handed dou-  
 62 blets and right-handed singlets. An important role for low-energy processes is played by the  
 63 charged weak current

$$J_{\text{cc}}^\alpha = \sum_\ell \bar{\nu}_\ell \gamma^\alpha P_L \ell + \sum_{ij} V_{ij} \bar{u}_i \gamma^\alpha P_L d_j, \quad (5.9)$$

64 which couples only to left-handed fermions,  $P_L \equiv (1 - \gamma_5)/2$ . In the sum over the quark-  
 65 field terms, the CKM matrix  $V_{ij}$  describes the flavor-changing effects of the weak interactions.  
 66 Including for completeness also the neutral weak current  $J_{\text{nc}}^\alpha$ , the interactions of (5.2) are  
 67 modified to

$$\mathcal{L}_{\text{EW}}^{\text{int}} = e A_\alpha J_{\text{em}}^\alpha + \frac{g}{\sqrt{2}} (W_\alpha^+ J_{\text{cc}}^\alpha + \text{h.c.}) + g_Z Z_\alpha J_{\text{nc}}^\alpha, \quad (5.10)$$

68 where  $g = e/\sin \theta_W$ ,  $g_Z = g/\cos \theta_W$  are the weak  $SU(2)_L$  couplings that can be expressed in  
 69 terms of  $e$  and the electroweak mixing (Weinberg) angle  $\theta_W$ . At the typical energy of processes  
 70 considered here, much smaller than  $m_W$  and  $m_Z$ , the  $W$  and  $Z$  boson masses, we can integrate  
 71 out the  $W$  and  $Z$  bosons and adopt an effective field theory (EFT) approach. This results in  
 72 the Fermi theory of current-current interactions

$$\mathcal{L}_{4F} = -\frac{4G_F}{\sqrt{2}} (J_{\text{cc}}^\alpha (J_{\text{cc}}^\alpha)^\dagger + J_{\text{nc}}^\alpha (J_{\text{nc}}^\alpha)_\alpha), \quad (5.11)$$

73 where  $4G_F/\sqrt{2} = g^2/(2m_W^2)$  is the matching (Wilson) coefficient at tree level. Using (5.9)  
 74 (and the corresponding expression for  $J_{\text{nc}}^\alpha$ ) to express  $\mathcal{L}_{4F}$  in terms of fermion fields we end  
 75 up with vector contact interactions. They correspond to dimension-6 four-fermion vector op-  
 76 erators of the generic form

$$[O_{\{\ell/q\}}^{V,XY}]_{ijkl} = (\bar{\psi}_i \gamma^\alpha P_X \psi_j) (\bar{\psi}_k \gamma_\alpha P_Y \psi_l), \quad (5.12)$$

77 where  $X, Y \in \{L, R\}$  and  $\{i, j, k, l\}$  are generation indices. The notion ‘vector’ refers to the  
 78 Lorentz structure of the bilinears, which in turn is closely related to the nature of the exchange  
 79 particle that is integrated out. Since the fermion fields  $\psi_i$  can be quarks or leptons of any  
 80 generation, there are in principle quite a lot of different operators. However, only a subset of  
 81 those are generated by integrating out the  $W$  and  $Z$  fields. In particular, there are no charged  
 82 lepton-flavor violating (cLFV) operators due to an accidental symmetry of the SM.

83 Because the masses of the top quark and the Higgs boson are of the same order as  $m_W$ ,  
 84 these fields can also be integrated out. Operators beyond the four-fermion vector operators  
 85 appear in the SM with an additional suppression, such as scalar dimension-6 four-fermion  
 86 operators

$$[O_{\{\ell/q\}}^{S,XY}]_{ijkl} = (\bar{\psi}_i P_X \psi_j) (\bar{\psi}_k P_Y \psi_l), \quad X, Y \in \{L, R\}, \quad (5.13)$$

87 which are parametrically suppressed by Yukawa couplings [24], or dimension-5 dipole opera-  
 88 tors (and their Hermitian conjugate)

$$[O_{\{\ell/q\}\gamma}^D]_{ij} = (\bar{\psi}_i \sigma_{\alpha\beta} P_R \psi_j) F^{\alpha\beta}, \quad [O_{qG}^D]_{ij} = (\bar{\psi}_i \sigma_{\alpha\beta} G^{\alpha\beta} P_R \psi_j), \quad (5.14)$$

89 which appear at the loop level. Thus, we arrive at an EFT that consistently describes low-  
 90 energy processes. It only contains fields with masses much lower than  $m_W$ . In particular, the  
 91 photon and the gluons are the only gauge bosons present. The gauge symmetry of the SM,  
 92  $SU(3)_c \times SU(2)_L \times U(1)_Y$ , is reduced to the gauge symmetry of QCD and QED,  $SU(3)_c \times U(1)_{\text{em}}$ .

93 The effect of the heavy degrees of freedom of the SM is encoded in the Wilson coefficients that  
 94 multiply the operators, with  $G_F$  in (5.11) being one such example.

95 In fact, this procedure lends itself to include possible BSM effects. Whatever BSM physics  
 96 there is, as long as it respects QED and QCD gauge symmetry and involves degrees of freedom  
 97 with a ‘large’ mass scale  $\Lambda$ , it can be integrated out and its effects will be encoded in Wilson  
 98 coefficients of gauge-invariant higher-dimensional operators. Operators that were absent in  
 99 the SM case might now be generated. Thus, we are led to write down the most general rela-  
 100 tivistic Lagrangian that respects electromagnetic  $U(1)_{\text{em}}$  and strong  $SU(3)_c$  gauge invariance  
 101 and obtain a general low-energy effective field theory (LEFT)

$$\mathcal{L}_{\text{LEFT}} = \mathcal{L}_{\text{QED+QCD}} + \frac{1}{\Lambda} \sum_i C_i^{(5)} O_i^{(5)} + \frac{1}{\Lambda^2} \sum_j C_j^{(6)} O_j^{(6)} + \dots \quad (5.15)$$

102 Here  $\Lambda$  is the scale of physics that is not dynamically described by the degrees of freedom  
 103 present in  $\mathcal{L}_{\text{LEFT}}$ . If we include all charged leptons and all quarks apart from the top in  $\mathcal{L}_{\text{LEFT}}$ ,  
 104 the scale  $\Lambda$  is assumed to be larger than the mass of the  $b$  quark but not larger than the  
 105 electroweak scale  $m_W$ . The sums  $i$  and  $j$  run over all possible operators of dimension 5 and  
 106 6, respectively. Typically, operators of dimension larger than 6 are neglected.  $O^{(5)}$  and  $O^{(6)}$   
 107 denote the operators,  $C^{(5)}$  and  $C^{(6)}$  are the corresponding Wilson coefficients. Operators that  
 108 are related through Fierz identities or those that can be eliminated through equations of motion  
 109 are not included. Naturally, the choice of the operator basis is not unique, but a complete basis  
 110 up to dimension 6 can be found in [24].

111 The Lagrangian (5.15) provides a consistent quantum-field theoretic framework to relate  
 112 low-energy measurements to the determination of parameters of the SM and constraints on  
 113 BSM physics. Many different routes have been taken to generically parametrize low-energy  
 114 observables and measuring or constraining the associated parameters. The prime example is  
 115 the Michel decay, where an analysis with initially a single parameter [25] was generalized and  
 116 written in terms of parameters related to scalar, vector and tensor contact interactions<sup>1</sup> [26].  
 117 A similar effort has been made for cLFV decays  $\mu \rightarrow e\gamma$  and  $\mu \rightarrow eee$  considering lepton-flavor-  
 118 violating contact interactions [27].

119 At first sight this is very similar to constraining the Wilson coefficients of (5.15). Indeed,  
 120 the bulk of the operators of (5.15) are also scalar, vector and tensor interactions. However, the  
 121 Wilson coefficients are well-defined couplings of a quantum field theory. In particular, typically  
 122 they run and mix under renormalization-group evolution (RGE). If a low-energy observable  
 123 is expressed in terms of Wilson coefficients, they are understood to be evaluated at the low  
 124 scale,  $C_i^{(n)}(m_\mu)$ . On the other hand, to relate the Wilson coefficients of the EFT to a BSM  
 125 model, the heavy degrees of freedom of the latter have to be integrated out. This yields the  
 126 Wilson coefficients at the high scale,  $C_i^{(n)}(\Lambda)$ . Including RGE of  $C_i^{(n)}(\Lambda)$  to  $C_i^{(n)}(m_\mu)$  is not in  
 127 the first instance about increasing precision, but to include qualitatively new effects through  
 128 mixing. This has a profound impact on using low-energy measurements to constrain BSM  
 129 models.

130 Of course, it is also possible that BSM physics appears only at a scale much larger than  
 131  $m_W$ . If this is the case, in a first step another effective theory has to be used, the SM effective  
 132 field theory (SMEFT). This is a theory similar to (5.15), but with all fields and symmetries of  
 133 the SM. It contains all operators  $O_i^{(n)}$  expressed in terms of the SM gauge fields, the Higgs  
 134 doublet, as well as left-handed doublet and right-handed singlet fermion fields that respect  
 135 the SM gauge symmetry  $SU(3)_c \times SU(2)_L \times U(1)_Y$ ,

$$\mathcal{L}_{\text{SMEFT}} = \mathcal{L}_{\text{SM}} + \frac{1}{\Lambda} (C^{(5)} O^{(5)} + \text{h.c.}) + \frac{1}{\Lambda^2} \sum_j C_j^{(6)} O_j^{(6)} + \dots \quad (5.16)$$

<sup>1</sup> Section 6: Muon decay [1]

136 SMEFT has only one dimension-5 operator  $\mathcal{O}^{(5)}$  (and its Hermitian conjugate). This is the  
 137 Weinberg operator [28] that is associated with neutrino masses. At dimension 6 there are  
 138 numerous operators, some of which violate baryon number. As for  $\mathcal{L}_{\text{LEFT}}$  different bases are  
 139 possible, but the so-called Warsaw basis [29] is used frequently.

140 In the case  $\Lambda \gg m_W$  the input of the BSM model is given through Wilson coefficients  
 141  $C_i^{(n)}(\Lambda)$ . Then, the RGE is used to obtain  $C_i^{(n)}(m_W)$ . In a next step, SMEFT is matched to  
 142 LEFT at the electroweak scale. This means that  $C_i^{(n)}(m_W)$  are expressed in terms of  $C_i^{(n)}(m_W)$ .  
 143 Finally, the Wilson coefficients of LEFT,  $C_i^{(n)}(m_W)$ , are run with the RGE of LEFT from the scale  
 144  $m_W$  to the low scale  $m_\mu$ , and we are ready to express physical low-energy observables. The  
 145 complete dimension-6 RGEs of SMEFT and LEFT, and the matching equations between the two  
 146 EFTs are known up to one loop [30–34].

147 Now that we have a framework that incorporates the effects of the full SM and potential  
 148 BSM physics on low-energy observables, we can return to our starting point, the matrix ele-  
 149 ments of the electromagnetic currents. Moving from (5.1) to (5.15) leads to a generalization  
 150 of (5.2), (5.3), and (5.5). In particular, the current itself is modified and includes additional  
 151 terms from the dimension-5 dipole operators. The most general expression for a vector current  
 152 depending on  $p_1$  and  $p_2$  can be written as combination of six possible structures:  $\gamma^\alpha$ ,  $\gamma^\alpha \gamma_5$ ,  $q^\alpha$ ,  
 153  $q^\alpha \gamma_5$ ,  $q_\beta \sigma^{\alpha\beta}$  and  $q_\beta \sigma^{\alpha\beta} \gamma_5$ . Replacing  $q = p_2 - p_1$  by  $p_2 + p_1$  does not lead to new independent  
 154 structures, as can be shown by using the Dirac equation. Since the electromagnetic current is  
 155 conserved  $\partial_\alpha J_{\text{em}}^\alpha = 0$  only four terms remain and we get

$$\begin{aligned} \langle f(p_2) | J_{\text{em}}^\alpha | f(p_1) \rangle = & \bar{u}(p_2, m_f) \left( F_1^{(f)}(q^2) \gamma^\alpha + (F_2^{(f)}(q^2) - i \gamma_5 F_3^{(f)}(q^2)) \frac{i \sigma^{\alpha\beta} q_\beta}{2m_f} \right. \\ & \left. + F_4^{(f)}(q^2) \frac{1}{m_f^2} (q^2 \gamma^\alpha - 2m_f q^\alpha) \gamma_5 \right) u(p_1, m_f). \end{aligned} \quad (5.17)$$

156 The CP-violating form factor  $F_3$  is associated with the electric dipole moment (EDM) of the  
 157 lepton  $d_f$  through

$$d_f = \frac{e F_3^{(f)}(0)}{2m_f}. \quad (5.18)$$

158 In the SM,  $d_f$  starts to receive contributions at three loops for quarks [35] and at four loops  
 159 for leptons [36], induced by the CP violation in the CKM matrix. For protons and neutrons  
 160 there is an additional source for an EDM [37] through the CP-violating  $\theta$  term in QCD

$$\mathcal{L}_{\text{QCD}} \supset \frac{g_s^2 \theta}{32\pi^2} \tilde{G}_{\alpha\beta} G^{\alpha\beta}, \quad (5.19)$$

161 which we have neglected in (5.1). This term has to be included as it respects  $SU(3)_c$  gauge  
 162 invariance. Even though it can be written as a total derivative and, so does not affect the  
 163 classical equations of motion, the  $\theta$  term does have effects at the quantum level. Thus strong  
 164 interactions seem to violate CP. However, due to experimental constraints on the neutron EDM,  
 165 we know that the  $\theta$  parameter is extremely small, see Section 5.6. The lack of an explanation  
 166 for this smallness is referred to as the strong CP problem. In generic BSM models, one usually  
 167 expects much larger CP-violating effects [38, 39]. The parity-violating anapole form factor  $F_4$  is  
 168 also induced due to weak interactions of the SM, or potentially through BSM effects. However,  
 169 it is not an observable by itself [40].

170 As mentioned above, matrix elements of the weak charged current  $J_{\text{cc}}^\alpha$  also play an impor-  
 171 tant role. It gives rise to non-vanishing matrix elements between different particles of left-  
 172 handed  $SU(2)$  doublets, such as  $(\nu_\ell, \ell)$  or  $(p, n)$ . The former leads to muon decay, whereas

173 the latter for example to beta decay, or quasi-elastic scattering  $\ell p \rightarrow \nu_\ell n$ . In this case, all six  
 174 structures appear and setting  $m_p = m_n \equiv m_N$  we have

$$\begin{aligned} \langle p(p_2) | J_{cc}^\alpha | n(p_1) \rangle = & \bar{u}(p_2, m_N) \left( F_1^{(pn)}(q^2) \gamma^\alpha + F_2^{(pn)}(q^2) \frac{i \sigma^{\alpha\beta} q_\beta}{2 m_N} + F_A^{(pn)}(q^2) \gamma^\alpha \gamma_5 \right. \\ & \left. + F_P^{(pn)}(q^2) \frac{q^\alpha \gamma_5}{2 m_N} + F_S^{(pn)}(q^2) \frac{q^\alpha}{m_N} + F_T^{(pn)}(q^2) \frac{i \sigma^{\alpha\beta} q_\beta \gamma_5}{2 m_N} \right) u(p_1, m_N). \end{aligned} \quad (5.20)$$

175 The scalar and tensor form factors  $F_S$  and  $F_T$  are referred to as second-class currents and often  
 176 are omitted. However, we will return to them in Section 5.6 in connection with the nucleon  
 177  $\beta^-$  decay, see (5.45), which can be related to  $F_{S,T}^{(pn)}$  and  $F_{S,T}^{(\nu_e e^-)}$ . The axial-vector and the  
 178 pseudoscalar form factors,  $F_A^{(pn)}$ , and  $F_P^{(pn)}$  are related to often used couplings as

$$g_A \equiv F_A^{(pn)}(0), \quad \bar{g}_A \equiv F_A^{(pn)}(q_0^2), \quad \bar{g}_P \equiv \frac{m_\mu}{m_N} F_P^{(pn)}(q_0^2), \quad (5.21)$$

179 where  $q_0^2 = -0.88 m_\mu^2$  is the momentum transfer of  $\mu^-$  capture on the proton, neglecting  
 180 binding energies.

181 Of course, not only the Wilson coefficients of the EFTs are subject to RGEs and thus scale  
 182 dependent, but also the gauge couplings  $\alpha = e^2/(4\pi)$  and  $\alpha_s = g_s^2/(4\pi)$  in (5.1). Both de-  
 183 pend on the energy of the phenomenon they are used to describe, but while  $\alpha(Q^2)$  decreases  
 184 towards  $\alpha(0) \sim 1/137$ , the strong coupling  $\alpha_s(Q^2)$  increases as we go to lower energies. For  
 185 energy scales below a couple of GeV, a perturbative expansion in  $\alpha_s$  no longer works — the rel-  
 186 evant degrees of freedom related to the strong interactions at low energies are not quarks and  
 187 gluons, but light hadrons. Once more, EFT come to the rescue, in this case chiral perturbation  
 188 theory ( $\chi$ PT) [41–43]. As for all EFT, the first step is to identify the relevant degrees of free-  
 189 dom in the energy range of interest. The second is to write down the most general Lagrangian  
 190 for these degrees of freedom that is compatible with the symmetries of the underlying theory.  
 191 For the strong interactions the answer to the first question is related to the phenomenon of  
 192 spontaneous chiral symmetry breaking, which generates Goldstone bosons, the only massless  
 193 particles of strong interactions. Actually in the spectrum of QCD there are no massless parti-  
 194 cles, but a triplet of very light pseudoscalars, the pions  $\vec{\pi} = (\pi^+, \pi^0, \pi^-)$ . The fact that they  
 195 are not exactly massless is well understood and due to the presence of an explicit, but small,  
 196 chiral symmetry breaking term in the QCD Lagrangian: the quark mass term. In the limit of  
 197 zero up and down quark masses, i.e.,  $m_d = m_u = 0$ , the three pions become massless, and  
 198 since there are no other mechanisms to generate massless particles in QCD in the chiral limit,  
 199 these are the only relevant degrees of freedom at low energy.

200 The rules to write down an effective Lagrangian for Goldstone bosons are well known.  
 201 Goldstone bosons transform nonlinearly under the symmetry of the underlying theory, which  
 202 leads to a non-renormalizable Lagrangian containing only derivative couplings. Symmetry  
 203 constrains their interaction to become weaker as one lowers the energy. How to include an  
 204 explicit symmetry breaking is also well known. The symmetry breaking parameters are pro-  
 205 moted to spurions, fields with given transformation laws, and the effective Lagrangian must  
 206 include these fields too and still satisfy the requirement of being invariant under symmetry  
 207 transformations. In the case of QCD, in addition to derivative couplings, it is also possible to  
 208 have couplings proportional to the quark masses  $m_{u,d}$ . Clearly, there are infinitely many such  
 209 terms and the Lagrangian only becomes useful with an organizing principle. Since this is a  
 210 low-energy EFT, we count powers of energy or momenta as small, and since it is relativistic,  
 211 they come in even powers. The smallest possible number is two, then four, six and so on.  
 212 Quark masses (or explicit symmetry breaking in general) also count as small, but there is no

213 unique choice concerning the relative importance of powers of quark masses and derivatives.  
 214 The standard one is  $m \sim p^2$ . According to this choice the lowest-order Lagrangian contains all  
 215 possible terms with two powers of derivatives or one power of quark masses and it turns out  
 216 that there are only two:

$$\mathcal{L}_{\chi\text{PT}} = \mathcal{L}_2 + \mathcal{L}_4 + \mathcal{L}_6 + \dots, \quad \mathcal{L}_2 = \frac{F^2}{4} \langle u_\mu u^\mu + \chi_+ \rangle, \quad (5.22)$$

217 where  $u_\mu = iu^\dagger \partial_\mu U u^\dagger$ ,  $\chi_+ = u^\dagger \chi u^\dagger + u \chi^\dagger u$ , and

$$U = uu = \exp(i\phi/F), \quad \phi = \pi^a \tau_a, \quad \chi = 2B \text{diag}(m_u, m_d), \quad (5.23)$$

218 with  $\pi^a$  the triplet of pion fields and  $\tau_a$  the Pauli matrices. The coupling constants charac-  
 219 terizing these two terms,  $F$  and  $B$ , are related to the pion decay constant and the pion mass  
 220 according to

$$\langle 0 | (J_A^a)_\mu(0) | \pi^b(p) \rangle = i\delta^{ab} F_\pi p_\mu, \quad F_\pi = F(1 + \mathcal{O}(m_q)), \quad M_\pi = 2B\hat{m}(1 + \mathcal{O}(m_q)), \quad (5.24)$$

221 with  $(J_A^a)_\mu$  the isospin-triplet axial current and  $\hat{m} = (m_u + m_d)/2$ . Calculating tree-level di-  
 222 agrams with  $\mathcal{L}_2$  gives a leading-order (LO) result. Going to next-to-leading order (NLO) re-  
 223 quires calculating one-loop diagrams with vertices only from  $\mathcal{L}_2$  and tree-level diagrams with  
 224 one vertex from  $\mathcal{L}_4$  [28, 42]. At next-to-next-to leading order (NNLO) two-loop diagrams with  
 225 vertices only from  $\mathcal{L}_2$ , one-loop diagrams with one vertex from  $\mathcal{L}_4$  and tree-level diagrams  
 226 with two vertices from  $\mathcal{L}_4$  or one from  $\mathcal{L}_6$  contribute [44–46], and so on.

227 The limit of validity of this EFT is given by the scale of chiral symmetry breaking. In  
 228 the expansion in powers of momenta and quark masses that is generated by the effective  
 229 Lagrangian above, the relevant scale is represented by  $\Lambda_\chi = 4\pi F_\pi \sim 1.2$  GeV. Physically it  
 230 represents the scale at which degrees of freedom other than Goldstone bosons get excited,  
 231 such as the  $\rho$ , whose mass  $m_\rho \sim 0.77$  GeV is indeed close to  $\Lambda_\chi$ .

232 The same approach also works for other particles beyond the pions. In the limit  $m_s \rightarrow 0$   
 233 also the kaons and the eta become Goldstone bosons and can be included in the formalism  
 234 above [47]. The field  $\phi$  becomes a  $3 \times 3$  matrix containing the octet of Goldstone bosons  
 235  $\phi = \phi^a \lambda_a$ , and  $\chi$  has to be trivially extended to a diagonal  $3 \times 3$  quark-mass matrix.

236 A less trivial extension concerns the baryon sector [48–51]. At first sight this would seem  
 237 impossible, since the mass of the nucleons is close to  $\Lambda_\chi$ . But the baryon number  $n_B$  is con-  
 238 served in strong interactions and one can split the spectrum in separated sectors, labeled by  
 239  $n_B$ . Quantities like the nucleon masses, their form factors, or their scattering amplitude with a  
 240 pion (or any other Goldstone boson(s)) all belong to the sector  $n_B = 1$  and can also be studied  
 241 with the help of the chiral expansion. In this case this represents an expansion in powers of  
 242 momenta and quark masses around the ground-state energy, which in this sector is equal to  
 243 the mass of the nucleon  $m_N$ , rather than zero.

244 From the point of view of their transformation properties, nucleons are spin-1/2 as well  
 245 as isospin-1/2 particles, and transform linearly under chiral transformations. In particular the  
 246 fact that they are spin-1/2 particles has an important consequence as the expansion of the  
 247 Lagrangian in powers of momenta (derivatives) contains both even and odd powers

$$\mathcal{L}_N = \mathcal{L}_1 + \mathcal{L}_2 + \mathcal{L}_3 + \dots \quad (5.25)$$

248 The leading-order Lagrangian looks as follows

$$\mathcal{L}_1 = \bar{N}(i\not{D} - m)N + \frac{1}{2} g_A \bar{N} \not{\psi} \gamma_5 N \quad (5.26)$$



249 with the covariant derivative defined as

$$D_\mu = \partial_\mu + \Gamma_\mu, \quad \Gamma_\mu = \frac{1}{2}[u^\dagger, \partial_\mu u], \quad (5.27)$$

250 and  $\bar{N} = (\bar{p}, \bar{n})$  the isospin doublet containing the Dirac spinors of the proton and neutron. The  
 251 parameters  $m$  and  $g_A$  represent the mass and the axial coupling of the nucleon in the chiral  
 252 limit, respectively. Note that the chiral symmetry imposes the presence of the pion field both  
 253 in the covariant derivative as well as in the coupling to the nucleon axial current. From this  
 254 follows the famous Golberger-Treiman relation [52]

$$g_{\pi N} = \frac{g_A m_N}{F_\pi} \quad (5.28)$$

255 between the pion-nucleon coupling constant  $g_{\pi N}$  (whose square is the residue of the nucleon  
 256 pole in the  $\pi N$  scattering amplitude), the physical nucleon mass, and the axial coupling.

257 The low-energy description of the strong-interaction effects in terms of  $\chi$ PT cannot only  
 258 be formulated for pure QCD as the underlying theory. While QED effects can be included in  
 259 terms of explicit low-energy degrees of freedom, the chiral realization of higher-dimensional  
 260 operators again is based on the external-field and spurion technique. Traditionally, this has  
 261 been done to include weak-interaction effects and it can be generalized to include BSM effects  
 262 encoded in the LEFT Lagrangian (5.15).

### 263 5.3 The muon

264 The muon is a fundamental lepton similar to the electron, however with a much larger mass,  
 265  $m_\mu \simeq 105.66 \text{ MeV}$ . It is unstable and predominantly decays through the Michel process

$$\mu \rightarrow e \nu \bar{\nu}, \quad (5.29)$$

266 which leads<sup>2</sup> to a lifetime of about  $\tau_\mu \simeq 2.2 \mu\text{s}$ . As discussed in the context of (5.20) the decay  
 267 is mediated by the charged current  $J_{\text{cc}}^\alpha$ , leading to a non-vanishing current-current interaction  
 268  $\langle \nu_\mu | J_{\text{cc}}^\alpha | \mu \rangle \langle e | (J_{\text{cc}}^\alpha)^\dagger | \nu_e \rangle$ . From an EFT point of view this corresponds to a four-fermion oper-  
 269 ator  $(\bar{\nu}_\mu \gamma^\alpha P_L \mu)(\bar{e} \gamma_\alpha P_L \nu_e)$  and its Hermitian conjugate. For computational reasons it is more  
 270 convenient to work with the Fierz transform of this operator. This results in the Fermi theory,  
 271 an EFT defined through the Lagrangian

$$\mathcal{L}_{\text{Fermi}} = -\frac{4 G_F}{\sqrt{2}} (\bar{\nu}_\mu \gamma_\alpha P_L \nu_e)(\bar{e} \gamma^\alpha P_L \mu) + \text{h.c.} + \mathcal{L}_{\text{QED}}. \quad (5.30)$$

272 The first term on the r.h.s. of (5.30) corresponds to the operator  $[O_{\nu\ell}^{V,LL}]_{2112}$  as introduced in  
 273 (5.12). Its Wilson coefficient,  $4 G_F / \sqrt{2}$ , has the special property that it does not get renormal-  
 274 ized [53]. Thus, the Lagrangian (5.30) can be used to consistently compute at leading order in  
 275  $G_F$  but to all orders in the electromagnetic coupling,  $\alpha$ . Only the usual QED renormalization  
 276 procedure has to be applied. As an example, the lifetime of the muon can be expressed as

$$\frac{1}{\tau_\mu} \equiv \Gamma_\mu = \Gamma_0(1 + \Delta q) = \frac{G_F^2 m_\mu^5}{192 \pi^3} (1 + \Delta q), \quad (5.31)$$

277 where  $\Delta q$  contains all corrections (electron-mass effects as well as higher-order QED cor-  
 278 rections) to the tree-level result for massless electrons,  $\Gamma_0$ . These corrections are known at  
 279 NNLO with full electron mass dependence [54–57]. Thus, with a precision measurement of

<sup>2</sup> Section 16: MuLan [2]

280 the muon lifetime, the Wilson coefficient in (5.30), or equivalently  $G_F$ , can be determined  
 281 extremely precisely. This, in turn, is important input for electroweak precision tests. In fact,  
 282  $G_F$  can be related to the  $SU(2)_L$  coupling  $g$  and the mass of the  $W$  boson  $m_W$  through

$$\frac{4G_F}{\sqrt{2}} = \frac{g^2}{2m_W^2}(1 + \Delta r). \quad (5.32)$$

283 While the SM radiative corrections  $\Delta r$  are crucial for the precision tests, the tree-level match-  
 284 ing of the SM to the Fermi theory yields the matching condition (5.32) with  $\Delta r \rightarrow 0$ .

285 There are several potentially numerically important contributions missing in (5.30). Typ-  
 286 ically,  $\mathcal{L}_{\text{QED}}$  contains muon and electron fields, but the inclusion of  $\tau$  leptons is straightfor-  
 287 ward. A much more serious issue is the inclusion of quarks. As mentioned above, QCD is non-  
 288 perturbative at scales typical for muonic processes,  $q^2 \sim m_\mu^2$ . Thus, the hadronic contributions  
 289 have to be determined by other means. This is often the leading theoretical uncertainty. The  
 290 fact that such corrections for muonic processes enter only at NNLO makes the muon a rather  
 291 clean laboratory for precision physics.

292 Furthermore, terms of order  $q^2/m_W^2$  relative to the four-fermion interaction are neglected  
 293 in (5.30) and typically in (5.15). In the literature (5.31) is often written with an additional  
 294 factor  $(1 + 3/5(m_\mu/m_W)^2)$  which results in a  $10^{-6}$  correction. Within the EFT, such correc-  
 295 tions are reproduced by dimension-8 operators, which are missing in (5.30). There are also  
 296 numerous dimension-6 operators generated by the SM that are not included in (5.30). The  
 297 corresponding Wilson coefficients are related to the general parametrization of muon decay  
 298 parameters.<sup>1</sup>

299 Apart from the Michel decay, two further SM decay processes are of interest; the radiative  
 300 and rare decays

$$\mu \rightarrow e \nu \bar{\nu} \gamma, \quad \mu \rightarrow e \nu \bar{\nu} e^+ e^-. \quad (5.33)$$

301 In order to be well defined and to avoid infrared singularities, the branching ratio for the radia-  
 302 tive decay must be defined requiring a minimal energy of the photon. For  $E_\gamma > 10$  MeV we have  
 303  $B(\mu \rightarrow e \nu \bar{\nu} \gamma) \sim 1.3 \times 10^{-2}$ . For the rare decay the branching ratio is  $B(\mu \rightarrow e \nu \bar{\nu} e e) \sim 3.6 \times 10^{-5}$ .  
 304 A fully differential NLO description of these processes in the Fermi theory (5.30) is avail-  
 305 able [58–61]. Depending on the cuts that are applied, the NLO QED corrections can be size-  
 306 able. Experimental information on the branching ratio of the radiative decay has been obtained  
 307 by MEG [62] and PiBeta [63].

308 A particularly attractive feature of particle physics with muons is the study of cLFV decays.  
 309 There are three "golden" channels

$$\mu \rightarrow e \gamma, \quad \mu \rightarrow e e e, \quad \mu^- \frac{A}{Z} N \rightarrow e^- \frac{A}{Z} N. \quad (5.34)$$

310 PSI has a long tradition in corresponding experimental searches.<sup>3,4,5,6</sup> For the first two pro-  
 311 cesses typically  $\mu^+$  are used, whereas  $\mu^-$  must be used for muon conversion in the field of a  
 312 nucleus  $\frac{A}{Z} N$  with atomic number  $Z$  and mass number  $A$ . In the SM (with non-vanishing neu-  
 313 trino masses) the branching ratios for these processes are smaller than  $10^{-50}$ , but not zero [64].  
 314 Hence, from a theory point of view there is nothing sacred about lepton flavor. As we know  
 315 that it is not conserved, it is very natural to expect much larger cLFV branching ratios in BSM  
 316 than in the SM. In fact, generic extensions of the SM do typically lead to large cLFV rates and  
 317 suppressing them requires additional tuning or model-building efforts.

<sup>3</sup> Section 7: Sindrum [3]

<sup>4</sup> Section 8: Sindrum II [4]

<sup>5</sup> Section 19: MEG [5]

<sup>6</sup> Section 20: Mu3e [6]

318 To extract constraints on BSM physics from limits on the branching ratios of the processes  
 319 (5.34), they are computed in  $\mathcal{L}_{\text{LEFT}}$ , typically at tree level. For  $\mu \rightarrow e\gamma$  the dipole operator  
 320  $[O_{\ell\gamma}^D]_{21}$  (5.14) enters. Thus we get a limit on the corresponding Wilson coefficient at the  
 321 low scale  $[C_{\ell\gamma}^D]_{21}(m_\mu)$ . In a next step, the RGE is used to convert this to limits for the Wilson  
 322 coefficients at the high scale,  $C_i(\Lambda)$ . Some scalar four-fermion interactions mix at NLO whereas  
 323 vector four-fermion interactions enter at NNLO. Nevertheless, this results in very stringent  
 324 limits on contact interactions induced by BSM physics. They have to be combined with limits  
 325 from  $\mu \rightarrow eee$  and muon conversion, where contact interactions already appear at leading  
 326 order. Using as many operators as possible in connection with RGE maximises the information  
 327 that can be obtained from low-energy observables.

328 These computations can be made [65] for  $\mu \rightarrow e\gamma$  and  $\mu \rightarrow eee$  using standard perturba-  
 329 tive methods with the Lagrangian (5.15), although for some contributions, non-perturbative  
 330 effects play a role [66]. However, additional input is required for muon conversion. First, the  
 331 nuclear matrix elements  $\langle {}^A_Z N | J | {}^A_Z N \rangle$  for vector and scalar currents/operators are required. The  
 332 former can be obtained trivially through current conversion, but the latter need input from  
 333 lattice QCD or  $\chi$ PT. Second, the overlap integrals of the lepton wave function with the nucleus  
 334 are required [67]. In principle different target nuclei provide different limits on the various  
 335 coefficients, but in practice the model discriminating power is limited [68]. A further compli-  
 336 cation is due to background from the decay in orbit (DIO). This is the Michel decay of the  $\mu^-$   
 337 bound in the nucleus

$$\mu^- \text{{}_Z^A N} \rightarrow e^- \nu_\mu \bar{\nu}_e \text{{}_Z^A N}. \quad (5.35)$$

338 Due to nuclear recoil effects the energy spectrum of the electron has a tail up to  $m_\mu$ , the  
 339 energy of the signal for the electron from muon conversion. Thus DIO has to be studied as a  
 340 background process [69].

341 So far the nucleus has acted only as a spectator. The only nuclear physics that was required  
 342 is the nuclear matrix element. For completeness we mention here two processes relevant to  
 343 muon conversion, where the nuclear physics is much more involved. When the  $\mu^-$  is bound to  
 344 the nucleus, it quickly cascades to the 1S ground state. Then it might undergo muon capture

$$\mu^- \text{{}_Z^A N} \rightarrow \nu_\mu \text{{}_{Z-1}^A N} \quad (5.36)$$

345 before it decays. The corresponding nuclear matrix element  $\langle {}_{Z-1}^A N | (J_{cc}^\alpha)^\dagger | {}_Z^A N \rangle$  is an extended  
 346 version of (5.20). It depends on the details of  ${}^A_Z N$  and is not easily accessible with theoretical  
 347 methods. We will return to muon capture in Section 5.4.

348 The muon can not only form bound states with a nucleus, but also with an electron. Muo-  
 349 nium,  $M = (\mu^+ e^-)$ , is a bound state like hydrogen, but with the proton replaced by a positive  
 350 muon. As the latter is a pointlike fermion, muonium is an excellent laboratory for QED tests,  
 351 and for a precise determination of the muon mass.<sup>7</sup> As the muonium mass is dominated by  
 352 antimatter,  $M$  is also an interesting option to study experimentally gravity of antimatter [70].  
 353 In addition, muonium-antimuonium oscillations

$$M = (\mu^+ e^-) \leftrightarrow \bar{M} = (\mu^- e^+), \quad (5.37)$$

354 which are forbidden in the SM, are another channel to scrutinize BSM physics.<sup>8</sup> A bound state  
 355 of two muons, true muonium  $(\mu^+ \mu^-)$ , is unfortunately, not experimentally accessible in the  
 356 foreseeable future.

357 Two further properties of the muon that are of utmost importance are the AMM (5.4) and  
 358 EDM (5.18). The motivation to study them in detail is again driven by the desire to test the

<sup>7</sup> Section 29: MSpec, Mu-Mass [7]

<sup>8</sup> Section 9: MACS [8]

359 SM. For the AMM very precise measurements are confronted with similarly precise theoretical  
 360 predictions [71]. At the time of writing, there is an intriguing tension between SM theory and  
 361 experiment. For the EDM, the situation is similar to cLFV searches in that the SM value is  
 362 zero for practical experimental purposes. Hence, experimental verification of a non-vanishing  
 363 muon EDM is a clear indication of BSM. So far, these quantities have not been measured by PSI  
 364 experiments. However, future involvement, in particular for the EDM, is being considered [72].

## 365 5.4 The proton

366 Like the electron and muon, the proton is a charged spin 1/2 fermion. However, because the  
 367 proton is a bound state, the form factors (5.5) cannot be computed perturbatively simply using  
 368  $\mathcal{L}_{\text{QED+QCD}}$ . Most information is obtained from experiment, with additional input from lattice  
 369 QCD and  $\chi\text{PT}$  [73]. From the charge and measurements of the AMM we know  $F_1^{(p)}(0) = 1$   
 370 and  $F_2^{(p)}(0) = \kappa_p \simeq 1.79$ .

371 A quantity that has received a lot of attention in the past years is the proton charge radius  
 372  $r_E^{(p)}$ . As discussed in the context of (5.8), the radius can be extracted as the slope of  $G_E^{(p)}(q^2)$   
 373 at  $q^2 \rightarrow 0$ . This can be determined by low- $q^2$  lepton-proton scattering with a careful  $q^2 \rightarrow 0$   
 374 extrapolation. An alternative approach is to use spectroscopy of normal hydrogen or better  
 375 muonic hydrogen. The overlap of the lepton wave function with the proton charge distribution  
 376 impacts on the energy levels. Thus, a precise measurement of different transition energies  
 377 allows the extraction of information on the proton radius. As the Bohr radius is proportional  
 378 to  $1/m_\ell$ , the effect in muonic atoms is considerably larger. This has resulted in a very precise  
 379 new determination of the proton radius<sup>9</sup> and a new world average of  $r_E^{(p)} \simeq 0.84$  fm. The  
 380 disagreement with earlier determinations of  $r_E^{(p)}$  was referred to as proton radius puzzle [74,  
 381 75], but the puzzle is fading away [76].

382 The CREMA collaboration<sup>9</sup> has measured two transition frequencies for muonic hydro-  
 383 gen; the triplet  $E(2P_{3/2}^{F=2}) - E(2S_{1/2}^{F=1})$  and singlet  $E(2P_{3/2}^{F=1}) - E(2S_{1/2}^{F=0})$ . From these two  
 384 values and theoretical input for the fine structure, it is possible to extract the Lamb shift  
 385  $E_L = E(2P_{1/2}) - E(2S_{1/2})$  and the hyperfine splitting  $E_{\text{HFS}} = E(2S_{1/2}^{F=1}) - E(2S_{1/2}^{F=0})$ . The  
 386 discrepancy of the proton radius determination from muonic hydrogen with earlier values  
 387 initiated a flurry of activities to revisit the theoretical calculations of the energy levels, as sum-  
 388 marized in [77]. This involves radiative corrections and recoil effects, which can in principle  
 389 be computed in perturbation theory.

390 In addition there are proton-structure effects, which are divided into two categories: a)  
 391 finite-size effects, which depend on the charge  $\rho_E$  and magnetic moment distribution  $\rho_M$  of  
 392 the proton, i.e., the charges related to the form factors  $G_E^{(p)}$  and  $G_M^{(p)}$ , introduced in (5.6); b)  
 393 polarizability effects.

394 The leading finite-size effect for  $E_L$  is in fact proportional to  $(r_E^{(p)})^2$  and it is precisely  
 395 this effect that allows an accurate determination of  $r_E^{(p)}$  from muonic hydrogen spectroscopy  
 396 to be made. There are also higher-order effects which have to be included, most notably a  
 397 contribution from the so-called third Zemach moment

$$(r_F^{(p)})^3 \equiv \frac{48}{\pi} \int_0^\infty \frac{dQ}{Q^4} \left( [G_E^{(p)}(Q^2)]^2 - 1 + \frac{1}{3} [r_E^{(p)}]^2 Q^2 \right), \quad (5.38)$$

398 where  $r_F^{(p)}$  is referred to as Friar radius. This contribution is related to the elastic two-photon  
 399 exchange (TPE), where elastic refers to the fact that the intermediate hadronic state is still a

<sup>9</sup> Section 21: CREMA [9]

400 proton. The inelastic TPE, i.e., TPE where the intermediate hadronic state is more complicated,  
 401 is often referred to as polarizability correction.

402 A similar distinction between perturbative and finite-size contributions can be made for the  
 403 hyperfine splitting  $E_{HFS}$ . In this case, the leading finite-size effect is proportional to the Zemach  
 404 radius  $r_Z^{(p)} \simeq 1.0$  fm, a convolution of the charge distribution with the magnetic moment  
 405 distribution

$$r_Z^{(p)} \equiv \int d^3\vec{r}_1 \int d^3\vec{r}_2 \rho_E^{(p)}(\vec{r}_1) \rho_M^{(p)}(\vec{r}_2) |\vec{r}_1 - \vec{r}_2|. \quad (5.39)$$

406 While the determination of the magnetic radius of the proton  $r_M^{(p)} \simeq 0.8$  fm was discussed  
 407 less controversially, there is also quite a spread in the values obtained from different extrac-  
 408 tions [78]. This spread is typically attributed to different treatment of TPE contributions.

409 The CREMA collaboration also investigated muonic deuterium and helium<sup>9</sup> and deter-  
 410 mined the corresponding charge radii. Measuring the charge radii of higher  $Z$  nuclei<sup>10</sup> pro-  
 411 vides crucial input for potential atomic parity violation experiments.

412 Returning to the proton, as mentioned above, studying lepton-proton scattering at low  $q^2$   
 413 is an important source to obtain information on the proton form factors and, hence, the proton  
 414 radius. At tree level, which implies the one-photon approximation, this process is described  
 415 by the famous Rosenbluth formula

$$\frac{d\sigma}{d\Omega} = \frac{\alpha^2}{4E_1^2 \sin^4 \theta_2} \frac{E_3}{E_1} \left( \frac{[G_E^{(p)}(q^2)]^2 + \tau [G_M^{(p)}(q^2)]^2}{1 + \tau} \cos^2 \theta_2 + 2\tau [G_M^{(p)}(q^2)]^2 \sin^2 \theta_2 \right) \quad (5.40)$$

416 in terms of  $\tau = -q^2/(4m_p^2)$ , the scattering angle  $\theta = 2\theta_2$ , and the energies of the incoming  
 417 and outgoing leptons,  $E_1$  and  $E_3$ , respectively. Using the standard dipole form  $G_D(q^2)$  for the  
 418 form factors gives a good fit to the experimental data:

$$G_E^{(p)}(q^2) \simeq \frac{G_M^{(p)}(q^2)}{1 + \kappa_p} \simeq G_D(q^2) = \frac{1}{(1 - q^2/\Lambda^2)^2} \quad \text{with } \Lambda^2 = 0.71 \text{ GeV}^2. \quad (5.41)$$

419 For very small  $q^2$  the form factors deviate from (5.41) and — coming back to the proton radius  
 420 issue — it is a delicate problem to extract the slope of the form factors in the limit  $q^2 \rightarrow 0$  from  
 421 scattering data.

422 Given the importance of lepton-proton scattering, there is a vast literature on the compu-  
 423 tation of higher-order corrections to (5.40). These corrections can be split into gauge inde-  
 424 pendent and finite subsets by separately considering radiative corrections from the lepton line,  
 425 radiation from the proton line, and multi-photon exchange between the proton and electron.

426 A full NLO calculation, superseding earlier ones where various approximations had been  
 427 used, has been presented in [79] and there are several Monte Carlo generators with these  
 428 corrections implemented [80, 81]. Corrections at NNLO due to radiation from the electron  
 429 line have also been computed [82, 83]. Due to the small mass of the lepton, these are the  
 430 dominant corrections, particularly for electron-proton scattering. As for spectroscopy, from a  
 431 theoretical point of view, multi-photon exchange contributions between the lepton and proton  
 432 are the most difficult ones to handle. Accordingly, TPE contributions have received a lot of  
 433 attention, also including the inelastic parts, see e.g. [84–87].

434 Traditionally, these experiments have been carried out with electrons. The MUSE collab-  
 435 oration<sup>11</sup> proposes to measure  $\ell p \rightarrow \ell p$  with  $\ell \in \{e^\pm, \mu^\pm\}$ . This offers the opportunity to

<sup>10</sup> Section 22: muX [10]

<sup>11</sup> Section 23: MUSE [11]

436 compare  $e p$  and  $\mu p$  scattering within the same experimental setup. In addition, experimen-  
 437 tal information on TPE can be obtained by measuring the difference between  $\ell^+ p$  and  $\ell^- p$   
 438 scattering.

439 To the best of our knowledge, the proton is a stable particle and in all processes discussed  
 440 so far, has been left intact. A low-energy process that affects the proton much more dramati-  
 441 cally is muon capture,  $\mu^- p \rightarrow n \nu_\mu$ . This process can be described by the transition matrix  
 442 element (5.20) as a current-current interaction  $\langle \nu_\mu | J_{cc}^\alpha | \mu \rangle \langle n | (J_{cc})_a^\dagger | p \rangle$ . In fact, muon capture  
 443 on the proton as measured by MuCap<sup>12</sup> gives valuable information on the corresponding form  
 444 factors, in particular  $\bar{g}_p$  (5.21) [88]. The inverse process would be related to neutrino-nucleon  
 445 scattering. Muon capture on the deuterium has been investigated by MuSun.<sup>13</sup>

## 446 5.5 Nucleons and nuclei

447 The proton and neutron together form an isospin doublet. They differ by their isospin projec-  
 448 tion,  $I_3 = +1/2$  and  $I_3 = -1/2$ , and quark content,  $uud$  and  $udd$ , respectively. The neutron's  
 449 Dirac and Pauli form factors are normalized as  $F_1^{(n)}(0) = 0$  and  $F_2^{(n)}(0) = \kappa_n \simeq -1.91$ . The  
 450 former differs from the proton form factor at zero momentum transfer,  $F_1^{(p)}(0) = 1$ , due to  
 451 the vanishing charge of the neutron. Therefore, the electric Sachs form factor of the neutron  
 452 cannot be approximated with a dipole form factor (5.41). Instead, the Galster form factor  
 453 could be used as a simple parametrization [89]:

$$G_E^{(n)}(q^2) = \frac{q^2 \kappa_n}{4m_n^2 - \eta q^2} G_D(q^2), \quad (5.42)$$

454 with  $\eta = 5.6$ . Since there are no free neutron targets, one has to rely on scattering off light  
 455 nuclei (e.g.,  $^2\text{H}$  or  $^3\text{He}$ ) to extract the neutron form factors and polarizabilities. Thereby, few-  
 456 nucleon EFTs are needed to separate the neutron from proton and nuclear effects.

457 As highlighted in the previous section, muonic atoms are sensitive to the nuclear structure.  
 458 The measurement of the muonic-hydrogen Lamb shift by the CREMA collaboration<sup>9</sup> allowed  
 459 the extraction of the proton root-mean-square charge radius with unprecedented precision.  
 460 From the measured the Lamb shifts in  $\mu\text{D}$ ,  $\mu^3\text{He}^+$  and  $\mu^4\text{He}^+$  the deuteron, helion and  $\alpha$ -  
 461 particle charge radii can be extracted. In the future, the ground-state hyperfine splitting of  
 462  $\mu^3\text{He}^+$  shall be measured to extract the helion Zemach radius. To extract the different nuclear  
 463 radii, precise theory predictions for the energy levels in muonic atoms are needed, see theory  
 464 summaries in [90–92]. Among other contributions, one needs the finite-size effects, through  
 465 which the different radii enter, and the polarizability effects. For the light muonic atoms,  
 466 not only the proton polarizability enters, but also the polarizabilities of the neutron and the  
 467 nucleus as a whole. Similar complications arise when going from pionic hydrogen to pionic  
 468 deuterium<sup>14</sup> or helium.<sup>15</sup> The nuclear polarizabilities are typically several orders of magni-  
 469 tude larger than the nucleon polarizabilities, and thus, more important. Take for instance  
 470 the electric dipole polarizability,  $\alpha_{E1}^{(n)} = 11.8(1.1) \times 10^{-4} \text{ fm}^3$  [93] and  $\alpha_{E1}^{(d)} = 0.6314(19)$   
 471  $\text{fm}^3$  [94], which describes the deformation of a composite particle in an external electric field  
 472 and gives a dominant contribution to the two-photon exchange. The nuclear polarizability  
 473 effects can be calculated in a dispersion relations framework [95, 96] or based on nuclear po-  
 474 tentials. For the latter, one distinguishes calculations with phenomenological models [97] fit  
 475 to nucleon-nucleon scattering data, such as the AV18 potential [98], or with nucleon-nucleon

<sup>12</sup> Section 17: MuCap [12]

<sup>13</sup> Section 18: MuSun [13]

<sup>14</sup> Section 14: Pionic hydrogen and deuterium [14]

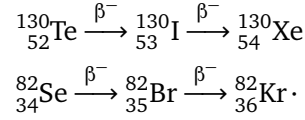
<sup>15</sup> Section 26: Pionic helium [15]

476 interactions derived from chiral EFT [99–102]. The nucleon-structure contributions are of-  
 477 ten deduced by rescaling the proton-structure contributions to  $\mu\text{H}$ . Take, for example, the  
 478 nucleon-polarizability contribution

$$\delta_{\text{pol}}^{\text{N}}(\mu\text{A}) = (\text{N} + \text{Z}) [Zm_r(\mu\text{A})/m_r(\mu\text{H})]^3 \delta_{\text{pol}}^{\text{N}}(\mu\text{H}), \quad (5.43)$$

479 where  $m_r$  is the reduced mass of the muonic atom and  $\text{Z}$ ,  $\text{N}$ ,  $\text{A}$  are the numbers of protons,  
 480 neutrons and nucleons in the nucleus.

481 Also in the field of muonic atoms, the muX project<sup>10</sup> determines nuclear charge radii of  
 482 radioactive elements and rare isotopes, e.g.  $^{248}\text{Cm}$  and  $^{226}\text{Ra}$ , through muonic X-ray measure-  
 483 ments. These are needed as input for atomic parity violation experiments. In addition, muX  
 484 probes nuclei that are at the end of a double  $\beta$  decay chain. These are interesting in view of  
 485 possible neutrinoless double  $\beta$  decay that could occur if neutrinos were Majorana particles.  
 486 Two examples are the following  $\beta^-\beta^-$  decays:



487 Here one uses muon capture to study excited states of  $^{130}\text{Xe}$  and  $^{82}\text{Kr}$ . In the future, direct  
 488 searches for BSM interactions between muons and nuclei might be possible with the muX  
 489 setup.

490 To further advance the precision of the few nucleon EFTs mentioned in this section, the  
 491 MuSun experiment<sup>13</sup> is studying muon-capture on deuterium:  $\mu^-d \rightarrow nn\nu_\mu$ . The aim is to  
 492 determine the low-energy constant (LEC) of the axial-vector four-nucleon interaction  $d$  [103]  
 493

$$\mathcal{L}_{NN} = -2d(N^\dagger S \cdot uN)N^\dagger N, \quad (5.44)$$

494 where  $S^\mu$  is the nucleon covariant spin operator,  $N(x)$  is the nucleon field, and  $u_\mu$  is given  
 495 below (5.22). Presently, this LEC has only been extracted from  $A = 3$  nuclei. The MuSun  
 496 experiment has the potential for an improved extraction at the 20% level.

## 497 5.6 The free neutron

498 In the previous section, we discussed nuclei and bound neutrons. In the following, we discuss  
 499 free neutrons provided by the Swiss Spallation Neutron Source (SINQ) and the PSI Ultra Cold  
 500 Neutron (UCN) source [104]. As we will see, the neutron experiments at PSI are dedicated to  
 501 BSM searches, and in particular, to the search for CP violation in the light quark sector.

502 The neutron is unstable with a lifetime of about 880 s. The long-standing tension between  
 503 measurements with in-flight and stored neutrons has led to speculations that there could be  
 504 ‘dark’ BSM decay channels [105, 106]. Within the SM, the neutron decays into the proton,  
 505 where the dominant decay channel is the classical  $\beta^-$  decay  $n \rightarrow pe^- \bar{\nu}_e$ , described by the  
 506 current-current interaction from the Fermi theory, (5.11). Besides the dominant  $V-A$  structure  
 507 of the weak interaction, there could be small admixtures of scalar and tensor couplings. Using  
 508 the general formulation of Lee and Yang, which is an older version of the parametrization in  
 509 (5.20), the  $\beta^-$  decay reads [107]

$$\begin{aligned} \langle pe^- \bar{\nu}_e | n \rangle = & \frac{G_F V_{ud}}{\sqrt{2}} \left[ \langle p | n \rangle \langle e^- | C_S - C'_S \gamma_5 | \nu_e \rangle + \langle p | \gamma_\mu | n \rangle \langle e^- | \gamma^\mu (C_V - C'_V \gamma_5) | \nu_e \rangle \right. \\ & + 1/2 \langle p | \sigma_{\lambda\mu} | n \rangle \langle e^- | \sigma^{\lambda\mu} (C_T - C'_T \gamma_5) | \nu_e \rangle - \langle p | \gamma_\mu \gamma_5 | n \rangle \langle e^- | \gamma^\mu \gamma_5 (C_A - C'_A \gamma_5) | \nu_e \rangle \\ & \left. + \langle p | \gamma_5 | n \rangle \langle e^- | \gamma_5 (C_P - C'_P \gamma_5) | \nu_e \rangle + \text{h.c.} \right], \quad (5.45) \end{aligned}$$

510 where  $C_i^{(\prime)}$  are 10 complex coupling constants. For the SM with conserved vector current,  
 511  $g_V = 1$ , the only non-vanishing couplings are  $C_V = C_V' = 1$  and  $C_A = C_A' = -g_A$ . Parity  
 512 violation is assured if  $C_i \neq 0$  and  $C_i' \neq 0$ . Time reversal violation (TRV), or CP violation, is  
 513 found if  $\text{Im}(C_i/C_j) \neq 0$  or  $\text{Im}(C_i'/C_j') \neq 0$ , i.e., if at least one coupling has an imaginary phase  
 514 relative to the others. The nTRV experiment<sup>16</sup> accessed the scalar and tensor couplings through  
 515 the measurement of the transverse polarization of electrons from the decay of polarized free  
 516 neutrons. At the present level of precision, the results are in agreement with the SM, thus,  
 517 setting constraints on BSM physics. For a review on electroweak SM tests with nuclear  $\beta$   
 518 decays see [108].

519 The observation of a nonzero permanent EDM of the neutron could be interpreted as a  
 520 signal of CP violating BSM interactions or a measurement of the QCD  $\theta$  parameter, see (5.19).  
 521 The current best limit  $|d_n| < 1.8 \times 10^{-26} e \text{ cm}$  is from the nEDM experiment<sup>17</sup> at PSI. This  
 522 limit is still compatible with the CKM-induced SM contributions to  $d_n$ , which are negligible as  
 523 explained below (5.18). The n2EDM experiment will improve the sensitivity to  $d_n$  by an order  
 524 of magnitude and probe BSM physics at the multi-TeV scale [39]. The electric field of these  
 525 experiments is of the order of  $10^6 \text{ V/m}$ . This is well below the critical electric field strength,  
 526  $E_{\text{crit.}} \sim 10^{23} \text{ V/m}$ , that would be able to induce an EDM proportional to the neutron electric  
 527 dipole polarizability  $d_{\text{ind.}} = 4\pi\alpha_{E1}\vec{E}$  [109]. The nEDM spectrometer has also been used in  
 528 indirect searches for Dark Matter (DM) candidates, e.g., mirror matter or axions and axion-  
 529 like particles (ALPs)<sup>18</sup>. The axion has been proposed as a dynamical solution to the strong  
 530 CP problem [110–113], i.e. the “naturalness” problem of the small QCD  $\theta$  parameter. It is  
 531 introduced as the Nambu-Goldstone boson associated with a spontaneously broken additional  
 532 global  $U(1)_{\text{PQ}}$  symmetry of the SM Lagrangian.

## 533 5.7 The pion

534 Low-energy pion physics provides access to a large variety of phenomena, ranging from strong  
 535 non-perturbative dynamics over electroweak precision tests to probes of BSM physics. The  
 536 pions are stable in pure QCD and as asymptotic QCD states they play a special role in many  
 537 hadronic processes, where they appear as hadronic final states. Pion interactions can be under-  
 538 stood beyond the chiral expansion by employing unitarity and analyticity of transition ampli-  
 539 tudes, which provide a means to resum pion-rescattering effects. Most notably,  $\pi\pi$  scattering  
 540 has been accurately described in terms of the Roy equations [114–116], and the resulting pre-  
 541 cise determination of the scattering phase shifts provides a central input in the analysis of a  
 542 host of other hadronic processes at low energies.

543 An important probe of QCD at low energies is provided by the interaction of pions with nu-  
 544 cleons. Pionic atoms provide access to  $S$ -wave  $\pi N$  scattering lengths [117], because the strong  
 545 interaction changes the spectrum compared to pure QED, resulting in shifts of the energy levels  
 546 and in finite widths of the bound state. The most precise measurements of pionic hydrogen and  
 547 deuterium have been performed at PSI.<sup>14</sup> The  $S$ -wave scattering lengths enter as important  
 548 constraints in a dispersive Roy–Steiner analysis of the  $\pi N$  scattering amplitude [118].

549 Compared to pure strong dynamics in the isospin limit, both electromagnetic effects and  
 550 the mass difference between up and down quarks generate small isospin-breaking corrections.  
 551 The mass difference of charged and neutral pions is understood to arise almost exclusively  
 552 from electromagnetic effects [42, 119, 120]. This mass difference  $m_{\pi^-} - m_{\pi^0}$  has been deter-  
 553 mined with high precision at PSI<sup>19</sup> starting from  $(\pi^- p)$  bound states with subsequent charge-  
 554 exchange reaction  $\pi^- p \rightarrow \pi^0 n$ .  $m_{\pi^-}$  has also been determined at PSI by measuring the energy

<sup>16</sup> Section 15: nTRV [16]

<sup>17</sup> Section 27: nEDM [17]

<sup>18</sup> Section 28: nEDMX [18]

<sup>19</sup> Section 12: neutral pions [21]



spectrum of pionic hydrogen ( $\pi^- p$ ).<sup>20</sup>

In the presence of electromagnetism, the neutral pion is not a stable particle, and decays predominantly into two photons. The decay results from the anomalous non-conservation of the axial current that couples to the pion. Quark-mass and electromagnetic corrections to the leading Adler–Bell–Jackiw anomaly have been worked out [121, 122]. Further decay modes, such as  $\pi^0 \rightarrow e^+ e^- \gamma$ ,  $\pi^0 \rightarrow 4e$ , and  $\pi^0 \rightarrow e^+ e^-$  involve the transition  $\pi^0 \rightarrow \gamma^* \gamma^{(*)}$  with one or two virtual photons. The transition form factor for this process has received considerable interest in connection with hadronic contributions to the muon anomalous magnetic moment [71, 123–125].

Charged pions only decay due to the weak interaction. The hadronic part of the decay rate for  $\pi^+ \rightarrow \ell^+ \nu_\ell$  is governed by the pion decay constant  $F_\pi$  of (5.24), whereas the leptonic part results in a helicity suppression by a factor  $m_\ell^2$ . Hence, the muonic decay mode dominates over the electronic mode and has been used to measure<sup>21</sup> the mass of  $\pi^+$ . Several other decay modes have been measured at PSI by the SINDRUM,<sup>3</sup> PiBeta,<sup>22</sup> and PEN<sup>23</sup> experiments, including the radiative decays  $\pi^+ \rightarrow \ell^+ \nu_\ell \gamma$  and  $\pi^+ \rightarrow e^+ \nu_e e^+ e^-$  and pion beta decay<sup>22</sup>  $\pi^+ \rightarrow \pi^0 e^+ \nu_e$ . The theoretical description of the radiative decay  $\pi^+ \rightarrow \ell^+ \nu_\ell \gamma$  is split into two parts, the so-called inner bremsstrahlung contributions (IB) and the structure-dependent terms (SD). The IB consist of the normal pion decay with additional emission of a photon from the charged external legs. This part depends on  $F_\pi$ . The SD terms require a more involved parametrization of the QCD effects in terms of two form factors. Apart from an axial form factor  $F_A$  also a vector form factor  $F_V$  contributes [126].

The charged-pion decays probe the weak interaction in the low-energy regime, where an excellent description is provided by Fermi’s effective theory of current-current interaction, or more generally the LEFT framework explained in Section 5.2. The relevant operator is

$$\mathcal{L}_{\text{LEFT}} \supset \sum_{i,j,k,l} C_{vedu}^{V,LL}{}_{ijkl} (\bar{\nu}_i \gamma^\alpha P_L \ell_j) (\bar{d}_k \gamma_\alpha P_L u_l) + \text{h.c.} \quad (5.46)$$

with flavor indices  $i, j, k, l$  and the SM tree-level matching at the weak scale given by  $C_{vedu}^{V,LL}{}_{ijkl} = -\frac{4G_F}{\sqrt{2}} \delta_{ij} V_{kl}^\dagger$ . Therefore, the pion decays probe the CKM matrix element  $V_{ud}$ , with a value of  $|V_{ud}| = 0.9739(27)$  resulting from the PiBeta measurement of pion beta decay. Although precise, this value is not competitive with determinations from superallowed nuclear beta decays [93], which currently are in some tension with first-row CKM unitarity. With the absence of nuclear structure aspects and with radiative corrections under good theoretical control [127], pion beta decays are theoretically clean but remain experimentally challenging due to the tiny branching ratio  $\sim 10^{-8}$ .

Additional semileptonic operators in the LEFT Lagrangian with different Dirac structures parametrize deviations from the SM and can be probed by several pion decay modes [128]. E.g., strong constraints on the first-generation tensor-operator coefficient  $\text{Re}(C_{vedu}^{T,RR})$  arise from the  $\pi^+ \rightarrow e^+ \nu_e \gamma$  Dalitz-plot study of the PiBeta experiment.

## 5.8 Conclusions

Low-energy, high-precision experiments provide essential input to improve our understanding of the fundamental interactions. They complement and extend information obtained from the energy frontier. EFTs are the theoretical tool of choice to describe and interpret their results and indeed they are well suited to describe both the SM and potential deviations therefrom

<sup>20</sup> Section 10: negative pions [19]

<sup>21</sup> Section 11: positive pions [20]

<sup>22</sup> Section 24: PiBeta [22]

<sup>23</sup> Section 25: PEN [23]

596 in a model-independent way. In particular it is possible, and crucial, to analyze if potential  
597 deviations from the SM in different observables are linked and have a common explanation.  
598 There are numerous examples where low-energy constraints rule out apparently attractive  
599 new physics scenarios. A broad and vigorous world-wide low-energy experimental program  
600 is indispensable to make further progress in testing the SM and searching for physics beyond.  
601 Past and future experiments at PSI will continue to play their part in this challenge.

## 602 References

- 603 [1] W. Fetscher, *Muon decay*, SciPost Phys. Proc. **2**, ppp (2021),  
604 doi:[10.21468/SciPostPhysProc.2.XXX](https://doi.org/10.21468/SciPostPhysProc.2.XXX).
- 605 [2] R. Carey, T. Goringe and D. Hertzog, *Mulan: a part-per-million measurement of the*  
606 *muon lifetime and determination of the Fermi constant*, SciPost Phys. Proc. **2**, ppp (2021),  
607 doi:[10.21468/SciPostPhysProc.2.XXX](https://doi.org/10.21468/SciPostPhysProc.2.XXX).
- 608 [3] R. Eichler and C. Grab, *The SINDRUM-I Experiment*, SciPost Phys. Proc. **2**, ppp (2021),  
609 doi:[10.21468/SciPostPhysProc.2.XXX](https://doi.org/10.21468/SciPostPhysProc.2.XXX).
- 610 [4] A. van der Schaaf, *Sindrum II*, SciPost Phys. Proc. **2**, ppp (2021),  
611 doi:[10.21468/SciPostPhysProc.2.XXX](https://doi.org/10.21468/SciPostPhysProc.2.XXX).
- 612 [5] A. Baldini and T. Mori, *MEG: Muon to Electron and Gamma*, SciPost Phys. Proc. **2**, ppp  
613 (2021), doi:[10.21468/SciPostPhysProc.2.XXX](https://doi.org/10.21468/SciPostPhysProc.2.XXX).
- 614 [6] F. Wauters, *The Mu3e experiment*, SciPost Phys. Proc. **2**, ppp (2021),  
615 doi:[10.21468/SciPostPhysProc.2.XXX](https://doi.org/10.21468/SciPostPhysProc.2.XXX).
- 616 [7] B. Ohayon, Z. Burkley and P. Crivelli, *Mspec: Muonium Spectroscopy*, SciPost Phys. Proc.  
617 **2**, ppp (2021), doi:[10.21468/SciPostPhysProc.2.XXX](https://doi.org/10.21468/SciPostPhysProc.2.XXX).
- 618 [8] K. Jungmann and L. Willmann, *Muonium-Antimuonium Conversion*, SciPost Phys. Proc.  
619 **2**, ppp (2021), doi:[10.21468/SciPostPhysProc.2.XXX](https://doi.org/10.21468/SciPostPhysProc.2.XXX).
- 620 [9] A. Antognini, *crema — t.b.c. ??*, SciPost Phys. Proc. **2**, ppp (2021),  
621 doi:[10.21468/SciPostPhysProc.2.XXX](https://doi.org/10.21468/SciPostPhysProc.2.XXX).
- 622 [10] F. Wauters and A. Knecht, *The muX project*, SciPost Phys. Proc. **2**, ppp (2021),  
623 doi:[10.21468/SciPostPhysProc.2.XXX](https://doi.org/10.21468/SciPostPhysProc.2.XXX).
- 624 [11] E. Downie, R. Gilman, J. Bernauer and E. Cline, *MUSE: The MUon Scattering Experiment*,  
625 SciPost Phys. Proc. **2**, ppp (2021), doi:[10.21468/SciPostPhysProc.2.XXX](https://doi.org/10.21468/SciPostPhysProc.2.XXX).
- 626 [12] M. Hildebrandt and C. Petitjean, *MuCap: Muon Capture on the Proton*, SciPost Phys.  
627 Proc. **2**, ppp (2021), doi:[10.21468/SciPostPhysProc.2.XXX](https://doi.org/10.21468/SciPostPhysProc.2.XXX).
- 628 [13] P. Kammel, *MuSun - Muon Capture on the Deuteron*, SciPost Phys. Proc. **2**, ppp (2021),  
629 doi:[10.21468/SciPostPhysProc.2.XXX](https://doi.org/10.21468/SciPostPhysProc.2.XXX).
- 630 [14] D. Gotta and L. Simons, *Pionic hydrogen and deuterium*, SciPost Phys. Proc. **2**, ppp  
631 (2021), doi:[10.21468/SciPostPhysProc.2.XXX](https://doi.org/10.21468/SciPostPhysProc.2.XXX).
- 632 [15] M. Hori, H. Aghai-Khozani, A. Sótér, A. Dax and D. Barna, *Recent results of laser spec-*  
633 *troscopy experiments of pionic helium atoms at PSI*, SciPost Phys. Proc. **2**, ppp (2021),  
634 doi:[10.21468/SciPostPhysProc.2.XXX](https://doi.org/10.21468/SciPostPhysProc.2.XXX).

- 635 [16] K. Bodek and A. Kozela, *Measurement of the transverse polarization of electrons*  
636 *emitted in neutron decay – nTRV experiment*, SciPost Phys. Proc. **2**, ppp (2021),  
637 doi:[10.21468/SciPostPhysProc.2.XXX](https://doi.org/10.21468/SciPostPhysProc.2.XXX).
- 638 [17] G. Pignol and P. Schmidt-Wellenburg, *The search for the neutron electric dipole moment*  
639 *at PSI*, SciPost Phys. Proc. **2**, ppp (2021), doi:[10.21468/SciPostPhysProc.2.XXX](https://doi.org/10.21468/SciPostPhysProc.2.XXX).
- 640 [18] S. Roccia and G. Zsigmond, *Indirect searches for dark matter with the nEDM spectrometer*,  
641 SciPost Phys. Proc. **2**, ppp (2021), doi:[10.21468/SciPostPhysProc.2.XXX](https://doi.org/10.21468/SciPostPhysProc.2.XXX).
- 642 [19] M. Daum and D. Gotta, *The mass of the  $\pi^-$* , SciPost Phys. Proc. **2**, ppp (2021),  
643 doi:[10.21468/SciPostPhysProc.2.XXX](https://doi.org/10.21468/SciPostPhysProc.2.XXX).
- 644 [20] M. Daum and P.-R. Kettle, *The mass of the  $\pi^+$* , SciPost Phys. Proc. **2**, ppp (2021),  
645 doi:[10.21468/SciPostPhysProc.2.XXX](https://doi.org/10.21468/SciPostPhysProc.2.XXX).
- 646 [21] M. Daum and P.-R. Kettle, *The  $\pi^0$  mass and the first experimental verification*  
647 *of Coulomb de-excitation in pinoic hydrogen*, SciPost Phys. Proc. **2**, ppp (2021),  
648 doi:[10.21468/SciPostPhysProc.2.XXX](https://doi.org/10.21468/SciPostPhysProc.2.XXX).
- 649 [22] D. Pocanic, *The pion beta and radiative electronic decays*, SciPost Phys. Proc. **2**, ppp  
650 (2021), doi:[10.21468/SciPostPhysProc.2.XXX](https://doi.org/10.21468/SciPostPhysProc.2.XXX).
- 651 [23] D. Pocanic, *Pion electronic decay and lepton universality*, SciPost Phys. Proc. **2**, ppp  
652 (2021), doi:[10.21468/SciPostPhysProc.2.XXX](https://doi.org/10.21468/SciPostPhysProc.2.XXX).
- 653 [24] E. E. Jenkins, A. V. Manohar and P. Stoffer, *Low-Energy Effective Field Theory*  
654 *below the Electroweak Scale: Operators and Matching*, JHEP **03**, 016 (2018),  
655 doi:[10.1007/JHEP03\(2018\)016](https://doi.org/10.1007/JHEP03(2018)016), [1709.04486](https://arxiv.org/abs/1709.04486).
- 656 [25] L. Michel, *Interaction between four half spin particles and the decay of the  $\mu$  meson*, Proc.  
657 Phys. Soc. **A63**, 514 (1950), doi:[10.1088/0370-1298/63/5/311](https://doi.org/10.1088/0370-1298/63/5/311), [,45(1949)].
- 658 [26] W. Fetscher, H. J. Gerber and K. F. Johnson, *Muon Decay: Complete Determination of*  
659 *the Interaction and Comparison with the Standard Model*, Phys. Lett. **B173**, 102 (1986),  
660 doi:[10.1016/0370-2693\(86\)91239-6](https://doi.org/10.1016/0370-2693(86)91239-6).
- 661 [27] Y. Kuno and Y. Okada, *Muon decay and physics beyond the standard model*, Rev. Mod.  
662 Phys. **73**, 151 (2001), doi:[10.1103/RevModPhys.73.151](https://doi.org/10.1103/RevModPhys.73.151), [hep-ph/9909265](https://arxiv.org/abs/hep-ph/9909265).
- 663 [28] S. Weinberg, *Baryon and Lepton Nonconserving Processes*, Phys. Rev. Lett. **43**, 1566  
664 (1979), doi:[10.1103/PhysRevLett.43.1566](https://doi.org/10.1103/PhysRevLett.43.1566).
- 665 [29] B. Grzadkowski, M. Iskrzynski, M. Misiak and J. Rosiek, *Dimension-Six Terms in the*  
666 *Standard Model Lagrangian*, JHEP **1010**, 085 (2010), doi:[10.1007/JHEP10\(2010\)085](https://doi.org/10.1007/JHEP10(2010)085),  
667 [1008.4884](https://arxiv.org/abs/1008.4884).
- 668 [30] E. E. Jenkins, A. V. Manohar and M. Trott, *Renormalization Group Evolution of the*  
669 *Standard Model Dimension Six Operators I: Formalism and lambda Dependence*, JHEP  
670 **1310**, 087 (2013), doi:[10.1007/JHEP10\(2013\)087](https://doi.org/10.1007/JHEP10(2013)087), [1308.2627](https://arxiv.org/abs/1308.2627).
- 671 [31] E. E. Jenkins, A. V. Manohar and M. Trott, *Renormalization Group Evolution of the Stan-*  
672 *dard Model Dimension Six Operators II: Yukawa Dependence*, JHEP **1401**, 035 (2014),  
673 doi:[10.1007/JHEP01\(2014\)035](https://doi.org/10.1007/JHEP01(2014)035), [1310.4838](https://arxiv.org/abs/1310.4838).

- 674 [32] R. Alonso, E. E. Jenkins, A. V. Manohar and M. Trott, *Renormalization Group Evolution of the Standard Model Dimension Six Operators III: Gauge Coupling Dependence and Phenomenology*, JHEP **1404**, 159 (2014), doi:[10.1007/JHEP04\(2014\)159](https://doi.org/10.1007/JHEP04(2014)159), [1312.2014](https://arxiv.org/abs/1312.2014).  
675  
676
- 677 [33] E. E. Jenkins, A. V. Manohar and P. Stoffer, *Low-Energy Effective Field Theory below the Electroweak Scale: Anomalous Dimensions*, JHEP **01**, 084 (2018),  
678 doi:[10.1007/JHEP01\(2018\)084](https://doi.org/10.1007/JHEP01(2018)084), [1711.05270](https://arxiv.org/abs/1711.05270).  
679
- 680 [34] W. Dekens and P. Stoffer, *Low-energy effective field theory below the electroweak scale: matching at one loop*, JHEP **10**, 197 (2019), doi:[10.1007/JHEP10\(2019\)197](https://doi.org/10.1007/JHEP10(2019)197), [1908.05295](https://arxiv.org/abs/1908.05295).  
681  
682
- 683 [35] A. Czarnecki and B. Krause, *Neutron electric dipole moment in the standard model: Valence quark contributions*, Phys. Rev. Lett. **78**, 4339 (1997),  
684 doi:[10.1103/PhysRevLett.78.4339](https://doi.org/10.1103/PhysRevLett.78.4339), [hep-ph/9704355](https://arxiv.org/abs/hep-ph/9704355).  
685
- 686 [36] M. E. Pospelov and I. B. Khriplovich, *Electric dipole moment of the W boson and the electron in the Kobayashi-Maskawa model*, Sov. J. Nucl. Phys. **53**, 638 (1991).  
687
- 688 [37] M. Pospelov and A. Ritz, *Theta induced electric dipole moment of the neutron via QCD sum rules*, Phys. Rev. Lett. **83**, 2526 (1999), doi:[10.1103/PhysRevLett.83.2526](https://doi.org/10.1103/PhysRevLett.83.2526), [hep-ph/9904483](https://arxiv.org/abs/hep-ph/9904483).  
689  
690
- 691 [38] M. Pospelov and A. Ritz, *Electric dipole moments as probes of new physics*, Annals Phys. **318**, 119 (2005), doi:[10.1016/j.aop.2005.04.002](https://doi.org/10.1016/j.aop.2005.04.002), [hep-ph/0504231](https://arxiv.org/abs/hep-ph/0504231).  
692
- 693 [39] J. Engel, M. J. Ramsey-Musolf and U. van Kolck, *Electric Dipole Moments of Nucleons, Nuclei, and Atoms: The Standard Model and Beyond*, Prog. Part. Nucl. Phys. **71**, 21  
694 (2013), doi:[10.1016/j.pnpnp.2013.03.003](https://doi.org/10.1016/j.pnpnp.2013.03.003), [1303.2371](https://arxiv.org/abs/1303.2371).  
695
- 696 [40] M. J. Musolf and B. R. Holstein, *Observability of the anapole moment and neutrino charge radius*, Phys. Rev. D **43**, 2956 (1991), doi:[10.1103/PhysRevD.43.2956](https://doi.org/10.1103/PhysRevD.43.2956).  
697
- 698 [41] S. Weinberg, *Phenomenological Lagrangians*, Physica A **96**(1-2), 327 (1979),  
699 doi:[10.1016/0378-4371\(79\)90223-1](https://doi.org/10.1016/0378-4371(79)90223-1).
- 700 [42] J. Gasser and H. Leutwyler, *Chiral Perturbation Theory to One Loop*, Annals Phys. **158**,  
701 142 (1984), doi:[10.1016/0003-4916\(84\)90242-2](https://doi.org/10.1016/0003-4916(84)90242-2).
- 702 [43] H. Leutwyler, *On the foundations of chiral perturbation theory*, Annals Phys. **235**, 165  
703 (1994), doi:[10.1006/aphy.1994.1094](https://doi.org/10.1006/aphy.1994.1094), [hep-ph/9311274](https://arxiv.org/abs/hep-ph/9311274).
- 704 [44] H. W. Fearing and S. Scherer, *Extension of the chiral perturbation theory meson Lagrangian to order  $p^6$* , Phys. Rev. D **53**, 315 (1996), doi:[10.1103/PhysRevD.53.315](https://doi.org/10.1103/PhysRevD.53.315),  
705 [hep-ph/9408346](https://arxiv.org/abs/hep-ph/9408346).  
706
- 707 [45] J. Bijnens, G. Colangelo and G. Ecker, *Renormalization of chiral perturbation theory to order  $p^6$* , Annals Phys. **280**, 100 (2000), doi:[10.1006/aphy.1999.5982](https://doi.org/10.1006/aphy.1999.5982), [hep-ph/9907333](https://arxiv.org/abs/hep-ph/9907333).  
708  
709
- 710 [46] J. Bijnens, G. Colangelo and G. Ecker, *The Mesonic chiral Lagrangian of order  $p^6$* ,  
711 JHEP **02**, 020 (1999), doi:[10.1088/1126-6708/1999/02/020](https://doi.org/10.1088/1126-6708/1999/02/020), [hep-ph/9902437](https://arxiv.org/abs/hep-ph/9902437).
- 712 [47] J. Gasser and H. Leutwyler, *Chiral Perturbation Theory: Expansions in the Mass of the Strange Quark*, Nucl. Phys. B **250**, 465 (1985), doi:[10.1016/0550-3213\(85\)90492-4](https://doi.org/10.1016/0550-3213(85)90492-4).  
713

- 714 [48] J. Gasser, M. E. Sainio and A. Svarc, *Nucleons with Chiral Loops*, Nucl. Phys. B **307**, 779  
715 (1988), doi:[10.1016/0550-3213\(88\)90108-3](https://doi.org/10.1016/0550-3213(88)90108-3).
- 716 [49] E. E. Jenkins and A. V. Manohar, *Baryon chiral perturbation theory using a heavy fermion*  
717 *Lagrangian*, Phys. Lett. B **255**, 558 (1991), doi:[10.1016/0370-2693\(91\)90266-S](https://doi.org/10.1016/0370-2693(91)90266-S).
- 718 [50] V. Bernard, N. Kaiser, J. Kambor and U. G. Meissner, *Chiral structure of the nucleon*,  
719 Nucl. Phys. B **388**, 315 (1992), doi:[10.1016/0550-3213\(92\)90615-I](https://doi.org/10.1016/0550-3213(92)90615-I).
- 720 [51] T. Becher and H. Leutwyler, *Baryon chiral perturbation theory in manifestly Lorentz*  
721 *invariant form*, Eur. Phys. J. C **9**, 643 (1999), doi:[10.1007/PL00021673](https://doi.org/10.1007/PL00021673), [hep-ph/](https://arxiv.org/abs/hep-ph/9901384)  
722 [9901384](https://arxiv.org/abs/hep-ph/9901384).
- 723 [52] M. L. Goldberger and S. B. Treiman, *Conserved Currents in the Theory of Fermi Interac-*  
724 *tions*, Phys. Rev. **110**, 1478 (1958), doi:[10.1103/PhysRev.110.1478](https://doi.org/10.1103/PhysRev.110.1478).
- 725 [53] S. Berman and A. Sirlin, *Some considerations on the radiative correc-*  
726 *tions to muon and neutron decay*, Annals of Physics **20**(1), 20 (1962),  
727 doi:[http://dx.doi.org/10.1016/0003-4916\(62\)90114-8](http://dx.doi.org/10.1016/0003-4916(62)90114-8).
- 728 [54] T. van Ritbergen and R. G. Stuart, *Complete two loop quantum electrodynamic con-*  
729 *tributions to the muon lifetime in the Fermi model*, Phys.Rev.Lett. **82**, 488 (1999),  
730 doi:[10.1103/PhysRevLett.82.488](https://doi.org/10.1103/PhysRevLett.82.488), [hep-ph/9808283](https://arxiv.org/abs/hep-ph/9808283).
- 731 [55] C. Anastasiou, K. Melnikov and F. Petriello, *The Electron energy spectrum in*  
732 *muon decay through  $O(\alpha^2)$* , JHEP **0709**, 014 (2007), doi:[10.1088/1126-](https://doi.org/10.1088/1126-6708/2007/09/014)  
733 [6708/2007/09/014](https://doi.org/10.1088/1126-6708/2007/09/014), [hep-ph/0505069](https://arxiv.org/abs/hep-ph/0505069).
- 734 [56] A. Pak and A. Czarnecki, *Mass effects in muon and semileptonic  $b \rightarrow c$  decays*, Phys. Rev.  
735 Lett. **100**, 241807 (2008), doi:[10.1103/PhysRevLett.100.241807](https://doi.org/10.1103/PhysRevLett.100.241807), [0803.0960](https://arxiv.org/abs/0803.0960).
- 736 [57] T. Engel, A. Signer and Y. Ulrich, *A subtraction scheme for massive QED*, JHEP **01**, 085  
737 (2020), doi:[10.1007/JHEP01\(2020\)085](https://doi.org/10.1007/JHEP01(2020)085), [JHEP20,085(2020)], [1909.10244](https://arxiv.org/abs/1909.10244).
- 738 [58] M. Fael, L. Mercolli and M. Passera, *Radiative  $\mu$  and  $\tau$  leptonic decays at NLO*, JHEP **07**,  
739 153 (2015), doi:[10.1007/JHEP07\(2015\)153](https://doi.org/10.1007/JHEP07(2015)153), [1506.03416](https://arxiv.org/abs/1506.03416).
- 740 [59] G. M. Pruna, A. Signer and Y. Ulrich, *Fully differential NLO predictions*  
741 *for the radiative decay of muons and taus*, Phys. Lett. **B772**, 452 (2017),  
742 doi:[10.1016/j.physletb.2017.07.008](https://doi.org/10.1016/j.physletb.2017.07.008), [1705.03782](https://arxiv.org/abs/1705.03782).
- 743 [60] G. M. Pruna, A. Signer and Y. Ulrich, *Fully differential NLO predictions for the rare muon*  
744 *decay*, Phys. Lett. **B765**, 280 (2017), doi:[10.1016/j.physletb.2016.12.039](https://doi.org/10.1016/j.physletb.2016.12.039), [1611.03617](https://arxiv.org/abs/1611.03617).
- 745 [61] M. Fael and C. Greub, *Next-to-leading order prediction for the decay  $\mu \rightarrow e(ee)\nu\bar{\nu}$* , JHEP  
746 **01**, 084 (2017), doi:[10.1007/JHEP01\(2017\)084](https://doi.org/10.1007/JHEP01(2017)084), [1611.03726](https://arxiv.org/abs/1611.03726).
- 747 [62] A. M. Baldini *et al.*, *Measurement of the radiative decay of polarized muons in the MEG*  
748 *experiment*, Eur. Phys. J. **C76**(3), 108 (2016), doi:[10.1140/epjc/s10052-016-3947-6](https://doi.org/10.1140/epjc/s10052-016-3947-6),  
749 [1312.3217](https://arxiv.org/abs/1312.3217).
- 750 [63] D. Pocanic *et al.*, *New results in rare allowed muon and pion decays*, Int. J. Mod. Phys.  
751 Conf. Ser. **35**, 1460437 (2014), doi:[10.1142/S2010194514604372](https://doi.org/10.1142/S2010194514604372), [1403.7416](https://arxiv.org/abs/1403.7416).
- 752 [64] S. T. Petcov, *The Processes  $\mu \rightarrow e + \gamma$ ,  $\mu \rightarrow e + \bar{e}$ ,  $\nu' \rightarrow \nu + \gamma$  in the Weinberg-Salam Model*  
753 *with Neutrino Mixing*, Sov. J. Nucl. Phys. **25**, 340 (1977), [Erratum: Sov. J. Nucl. Phys.  
754 **25**, 698 (1977), Erratum: Yad. Fiz. **25**, 1336 (1977)].

- 755 [65] A. Crivellin, S. Davidson, G. M. Pruna and A. Signer, *Renormalisation-group improved*  
756 *analysis of  $\mu \rightarrow e$  processes in a systematic effective-field-theory approach*, JHEP **05**, 117  
757 (2017), doi:[10.1007/JHEP05\(2017\)117](https://doi.org/10.1007/JHEP05(2017)117), [1702.03020](https://arxiv.org/abs/1702.03020).
- 758 [66] W. Dekens, E. E. Jenkins, A. V. Manohar and P. Stoffer, *Non-perturbative effects in  $\mu \rightarrow e\gamma$* ,  
759 JHEP **01**, 088 (2019), doi:[10.1007/JHEP01\(2019\)088](https://doi.org/10.1007/JHEP01(2019)088), [1810.05675](https://arxiv.org/abs/1810.05675).
- 760 [67] R. Kitano, M. Koike and Y. Okada, *Detailed calculation of lepton flavor violating*  
761 *muon electron conversion rate for various nuclei*, Phys. Rev. **D66**, 096002 (2002),  
762 doi:[10.1103/PhysRevD.76.059902](https://doi.org/10.1103/PhysRevD.76.059902), [10.1103/PhysRevD.66.096002](https://doi.org/10.1103/PhysRevD.66.096002), [Erratum: Phys.  
763 Rev.D76,059902(2007)], [hep-ph/0203110](https://arxiv.org/abs/hep-ph/0203110).
- 764 [68] V. Cirigliano, R. Kitano, Y. Okada and P. Tuzon, *On the model discriminat-*  
765 *ing power of  $\mu \rightarrow e$  conversion in nuclei*, Phys. Rev. **D80**, 013002 (2009),  
766 doi:[10.1103/PhysRevD.80.013002](https://doi.org/10.1103/PhysRevD.80.013002), [0904.0957](https://arxiv.org/abs/0904.0957).
- 767 [69] A. Czarnecki, M. Dowling, X. Garcia i Tormo, W. J. Marciano and R. Szafron, *Michel*  
768 *decay spectrum for a muon bound to a nucleus*, Phys. Rev. **D90**(9), 093002 (2014),  
769 doi:[10.1103/PhysRevD.90.093002](https://doi.org/10.1103/PhysRevD.90.093002), [1406.3575](https://arxiv.org/abs/1406.3575).
- 770 [70] A. Antognini, D. M. Kaplan, K. Kirch, A. Knecht, D. C. Mancini, J. D. Phillips, T. J.  
771 Phillips, R. D. Reasenberg, T. J. Roberts and A. Soter, *Studying Antimatter Gravity with*  
772 *Muonium*, Atoms **6**(2), 17 (2018), doi:[10.3390/atoms6020017](https://doi.org/10.3390/atoms6020017), [1802.01438](https://arxiv.org/abs/1802.01438).
- 773 [71] T. Aoyama *et al.*, *The anomalous magnetic moment of the muon in the Standard Model*,  
774 Phys. Rept. **887**, 1 (2020), doi:[10.1016/j.physrep.2020.07.006](https://doi.org/10.1016/j.physrep.2020.07.006), [2006.04822](https://arxiv.org/abs/2006.04822).
- 775 [72] K. Kirch and P. Schmidt-Wellenburg, *Search for electric dipole moments*, EPJ Web Conf.  
776 **234**, 01007 (2020), doi:[10.1051/epjconf/202023401007](https://doi.org/10.1051/epjconf/202023401007), [2003.00717](https://arxiv.org/abs/2003.00717).
- 777 [73] C. F. Perdrisat, V. Punjabi and M. Vanderhaeghen, *Nucleon Electromagnetic Form Factors*,  
778 Prog. Part. Nucl. Phys. **59**, 694 (2007), doi:[10.1016/j.pnpnp.2007.05.001](https://doi.org/10.1016/j.pnpnp.2007.05.001), [hep-ph/  
779 0612014](https://arxiv.org/abs/hep-ph/0612014).
- 780 [74] R. Pohl, R. Gilman, G. A. Miller and K. Pachucki, *Muonic hydrogen and the proton radius*  
781 *puzzle*, Ann. Rev. Nucl. Part. Sci. **63**, 175 (2013), doi:[10.1146/annurev-nucl-102212-  
782 170627](https://doi.org/10.1146/annurev-nucl-102212-170627), [1301.0905](https://arxiv.org/abs/1301.0905).
- 783 [75] C. E. Carlson, *The Proton Radius Puzzle*, Prog. Part. Nucl. Phys. **82**, 59 (2015),  
784 doi:[10.1016/j.pnpnp.2015.01.002](https://doi.org/10.1016/j.pnpnp.2015.01.002), [1502.05314](https://arxiv.org/abs/1502.05314).
- 785 [76] H.-W. Hammer and U.-G. Meißner, *The proton radius: From a puzzle to precision*, Sci.  
786 Bull. **65**, 257 (2020), doi:[10.1016/j.scib.2019.12.012](https://doi.org/10.1016/j.scib.2019.12.012), [1912.03881](https://arxiv.org/abs/1912.03881).
- 787 [77] A. Antognini, F. Kottmann, F. Biraben, P. Indelicato, F. Nez and R. Pohl, *Theory of the*  
788 *2S-2P Lamb shift and 2S hyperfine splitting in muonic hydrogen*, Annals Phys. **331**, 127  
789 (2013), doi:[10.1016/j.aop.2012.12.003](https://doi.org/10.1016/j.aop.2012.12.003), [1208.2637](https://arxiv.org/abs/1208.2637).
- 790 [78] J. M. Alarcón, D. W. Higinbotham and C. Weiss, *Precise determination of the proton*  
791 *magnetic radius from electron scattering data*, Phys. Rev. C **102**(3), 035203 (2020),  
792 doi:[10.1103/PhysRevC.102.035203](https://doi.org/10.1103/PhysRevC.102.035203), [2002.05167](https://arxiv.org/abs/2002.05167).
- 793 [79] L. C. Maximon and J. A. Tjon, *Radiative corrections to electron-proton scattering*, Physical  
794 Review C **62**(5) (2000), doi:[10.1103/physrevc.62.054320](https://doi.org/10.1103/physrevc.62.054320).

- 795 [80] A. Gramolin, V. Fadin, A. Feldman, R. Gerasimov, D. Nikolenko, I. Rachek and  
796 D. Toporkov, *A new event generator for the elastic scattering of charged leptons on pro-*  
797 *tons*, J. Phys. G **41**(11), 115001 (2014), doi:[10.1088/0954-3899/41/11/115001](https://doi.org/10.1088/0954-3899/41/11/115001),  
798 [1401.2959](https://arxiv.org/abs/1401.2959).
- 799 [81] I. Akushevich, H. Gao, A. Ilyichev and M. Meziane, *Radiative corrections beyond the ultra*  
800 *relativistic limit in unpolarized ep elastic and Møller scatterings for the PRad Experiment at*  
801 *Jefferson Laboratory*, Eur. Phys. J. A **51**(1), 1 (2015), doi:[10.1140/epja/i2015-15001-8](https://doi.org/10.1140/epja/i2015-15001-8).
- 802 [82] R.-D. Bucoveanu and H. Spiesberger, *Second-Order Leptonic Radiative Corrections for*  
803 *Lepton-Proton Scattering*, Eur. Phys. J. A **55**(4), 57 (2019), doi:[10.1140/epja/i2019-](https://doi.org/10.1140/epja/i2019-12727-1)  
804 [12727-1](https://arxiv.org/abs/1811.04970), [1811.04970](https://arxiv.org/abs/1811.04970).
- 805 [83] P. Banerjee, T. Engel, A. Signer and Y. Ulrich, *QED at NNLO with McMule*, SciPost Phys.  
806 **9**, 027 (2020), doi:[10.21468/SciPostPhys.9.2.027](https://doi.org/10.21468/SciPostPhys.9.2.027), [2007.01654](https://arxiv.org/abs/2007.01654).
- 807 [84] C. E. Carlson and M. Vanderhaeghen, *Two-Photon Physics in Hadronic Processes*, Ann.  
808 Rev. Nucl. Part. Sci. **57**, 171 (2007), doi:[10.1146/annurev.nucl.57.090506.123116](https://doi.org/10.1146/annurev.nucl.57.090506.123116),  
809 [hep-ph/0701272](https://arxiv.org/abs/hep-ph/0701272).
- 810 [85] J. Arrington, P. Blunden and W. Melnitchouk, *Review of two-photon exchange in electron*  
811 *scattering*, Prog. Part. Nucl. Phys. **66**, 782 (2011), doi:[10.1016/j.ppnp.2011.07.003](https://doi.org/10.1016/j.ppnp.2011.07.003),  
812 [1105.0951](https://arxiv.org/abs/1105.0951).
- 813 [86] A. Afanasev, P. Blunden, D. Hasell and B. Raue, *Two-photon exchange in*  
814 *elastic electron-proton scattering*, Prog. Part. Nucl. Phys. **95**, 245 (2017),  
815 doi:[10.1016/j.ppnp.2017.03.004](https://doi.org/10.1016/j.ppnp.2017.03.004), [1703.03874](https://arxiv.org/abs/1703.03874).
- 816 [87] O. Tomalak, B. Pasquini and M. Vanderhaeghen, *Two-photon exchange contribution to*  
817 *elastic  $e^-$ -proton scattering: Full dispersive treatment of  $\pi N$  states and comparison with*  
818 *data*, Phys. Rev. D **96**(9), 096001 (2017), doi:[10.1103/PhysRevD.96.096001](https://doi.org/10.1103/PhysRevD.96.096001), [1708.](https://arxiv.org/abs/1708.03303)  
819 [03303](https://arxiv.org/abs/1708.03303).
- 820 [88] R. J. Hill, P. Kammel, W. J. Marciano and A. Sirlin, *Nucleon Axial Radius and Muonic*  
821 *Hydrogen — A New Analysis and Review*, Rept. Prog. Phys. **81**(9), 096301 (2018),  
822 doi:[10.1088/1361-6633/aac190](https://doi.org/10.1088/1361-6633/aac190), [1708.08462](https://arxiv.org/abs/1708.08462).
- 823 [89] S. Galster, H. Klein, J. Moritz, K. H. Schmidt, D. Wegener and J. Bleckwenn, *Elastic*  
824 *electron-deuteron scattering and the electric neutron form factor at four-momentum*  
825 *transfers  $5\text{fm}^{-2} < q^2 < 14\text{fm}^{-2}$* , Nucl. Phys. B **32**, 221 (1971), doi:[10.1016/0550-](https://doi.org/10.1016/0550-3213(71)90068-X)  
826 [3213\(71\)90068-X](https://arxiv.org/abs/3213(71)90068-X).
- 827 [90] J. J. Krauth, M. Diepold, B. Franke, A. Antognini, F. Kottmann and R. Pohl, *Theory of the  $n=2$  levels in muonic deuterium*, Annals Phys. **366**, 168 (2016),  
828 doi:[10.1016/j.aop.2015.12.006](https://doi.org/10.1016/j.aop.2015.12.006), [1506.01298](https://arxiv.org/abs/1506.01298).  
829
- 830 [91] B. Franke, J. J. Krauth, A. Antognini, M. Diepold, F. Kottmann and R. Pohl, *Theory of the  $n = 2$  levels in muonic helium-3 ions*, Eur. Phys. J. D **71**(12), 341 (2017),  
831 doi:[10.1140/epjd/e2017-80296-1](https://doi.org/10.1140/epjd/e2017-80296-1), [1705.00352](https://arxiv.org/abs/1705.00352).  
832
- 833 [92] M. Diepold, B. Franke, J. J. Krauth, A. Antognini, F. Kottmann and R. Pohl, *Theory of*  
834 *the Lamb shift and Fine Structure in muonic  $^4\text{He}$  ions and the muonic  $^3\text{He} - ^4\text{He}$  Isotope*  
835 *Shift*, Annals Phys. **396**, 220 (2018), doi:[10.1016/j.aop.2018.07.015](https://doi.org/10.1016/j.aop.2018.07.015), [1606.05231](https://arxiv.org/abs/1606.05231).
- 836 [93] P. A. Zyla et al., *Review of Particle Physics*, PTEP **2020**(8), 083C01 (2020),  
837 doi:[10.1093/ptep/ptaa104](https://doi.org/10.1093/ptep/ptaa104).

- 838 [94] D. R. Phillips, G. Rupak and M. J. Savage, *Improving the convergence of  $NN$  effective*  
839 *field theory*, Phys. Lett. B **473**, 209 (2000), doi:[10.1016/S0370-2693\(99\)01496-3](https://doi.org/10.1016/S0370-2693(99)01496-3),  
840 [nucl-th/9908054](https://arxiv.org/abs/nucl-th/9908054).
- 841 [95] C. E. Carlson, M. Gorchtein and M. Vanderhaeghen, *Nuclear structure contribu-*  
842 *tion to the Lamb shift in muonic deuterium*, Phys. Rev. A **89**(2), 022504 (2014),  
843 doi:[10.1103/PhysRevA.89.022504](https://doi.org/10.1103/PhysRevA.89.022504), [1311.6512](https://arxiv.org/abs/1311.6512).
- 844 [96] C. E. Carlson, M. Gorchtein and M. Vanderhaeghen, *Two-photon exchange correc-*  
845 *tion to  $2S - 2P$  splitting in muonic  $^3\text{He}$  ions*, Phys. Rev. A **95**(1), 012506 (2017),  
846 doi:[10.1103/PhysRevA.95.012506](https://doi.org/10.1103/PhysRevA.95.012506), [1611.06192](https://arxiv.org/abs/1611.06192).
- 847 [97] K. Pachucki and A. Wienczek, *Nuclear structure effects in light muonic atoms*, Phys. Rev.  
848 A **91**(4), 040503 (2015), doi:[10.1103/PhysRevA.91.040503](https://doi.org/10.1103/PhysRevA.91.040503), [1501.07451](https://arxiv.org/abs/1501.07451).
- 849 [98] R. B. Wiringa, V. G. J. Stoks and R. Schiavilla, *An Accurate nucleon-nucleon*  
850 *potential with charge independence breaking*, Phys. Rev. C **51**, 38 (1995),  
851 doi:[10.1103/PhysRevC.51.38](https://doi.org/10.1103/PhysRevC.51.38), [nucl-th/9408016](https://arxiv.org/abs/nucl-th/9408016).
- 852 [99] C. Ji, N. Nevo Dinur, S. Bacca and N. Barnea, *Nuclear Polarization Cor-*  
853 *rections to the  $\mu^4\text{He}^+$  Lamb Shift*, Phys. Rev. Lett. **111**, 143402 (2013),  
854 doi:[10.1103/PhysRevLett.111.143402](https://doi.org/10.1103/PhysRevLett.111.143402), [1307.6577](https://arxiv.org/abs/1307.6577).
- 855 [100] O. J. Hernandez, C. Ji, S. Bacca, N. Nevo Dinur and N. Barnea, *Improved esti-*  
856 *mates of the nuclear structure corrections in  $\mu D$* , Phys. Lett. B **736**, 344 (2014),  
857 doi:[10.1016/j.physletb.2014.07.039](https://doi.org/10.1016/j.physletb.2014.07.039), [1406.5230](https://arxiv.org/abs/1406.5230).
- 858 [101] N. Nevo Dinur, C. Ji, S. Bacca and N. Barnea, *Nuclear structure correc-*  
859 *tions to the Lamb shift in  $\mu^3\text{He}^+$  and  $\mu^3\text{H}$* , Phys. Lett. B **755**, 380 (2016),  
860 doi:[10.1016/j.physletb.2016.02.023](https://doi.org/10.1016/j.physletb.2016.02.023), [1512.05773](https://arxiv.org/abs/1512.05773).
- 861 [102] C. Ji, S. Bacca, N. Barnea, O. J. Hernandez and N. Nevo-Dinur, *Abinitio calculation*  
862 *of nuclear structure corrections in muonic atoms*, J. Phys. G **45**(9), 093002 (2018),  
863 doi:[10.1088/1361-6471/aad3eb](https://doi.org/10.1088/1361-6471/aad3eb), [1806.03101](https://arxiv.org/abs/1806.03101).
- 864 [103] S. Pastore, F. Myhrer and K. Kubodera, *An update of muon capture on hydrogen*, Int.  
865 J. Mod. Phys. E **23**(08), 1430010 (2014), doi:[10.1142/S0218301314300100](https://doi.org/10.1142/S0218301314300100), [1405.](https://arxiv.org/abs/1405.1358)  
866 [1358](https://arxiv.org/abs/1358).
- 867 [104] B. Lauss and B. Blau, *UCN, the ultracold neutron source – neutrons for particle physics*,  
868 SciPost Phys. Proc. **2**, ppp (2021), doi:[10.21468/SciPostPhysProc.2.XXX](https://doi.org/10.21468/SciPostPhysProc.2.XXX).
- 869 [105] B. Fornal and B. Grinstein, *Dark Matter Interpretation of the Neutron Decay Anomaly*,  
870 Phys. Rev. Lett. **120**(19), 191801 (2018), doi:[10.1103/PhysRevLett.120.191801](https://doi.org/10.1103/PhysRevLett.120.191801), [Er-  
871 ratum: Phys.Rev.Lett. 124, 219901 (2020)], [1801.01124](https://arxiv.org/abs/1801.01124).
- 872 [106] A. Czarnecki, W. J. Marciano and A. Sirlin, *Neutron Lifetime and Axial Coupling Connec-*  
873 *tion*, Phys. Rev. Lett. **120**(20), 202002 (2018), doi:[10.1103/PhysRevLett.120.202002](https://doi.org/10.1103/PhysRevLett.120.202002),  
874 [1802.01804](https://arxiv.org/abs/1802.01804).
- 875 [107] T. D. Lee and C.-N. Yang, *Question of Parity Conservation in Weak Interactions*, Phys.  
876 Rev. **104**, 254 (1956), doi:[10.1103/PhysRev.104.254](https://doi.org/10.1103/PhysRev.104.254).
- 877 [108] N. Severijns, M. Beck and O. Naviliat-Cuncic, *Tests of the standard electroweak model*  
878 *in beta decay*, Rev. Mod. Phys. **78**, 991 (2006), doi:[10.1103/RevModPhys.78.991](https://doi.org/10.1103/RevModPhys.78.991),  
879 [nucl-ex/0605029](https://arxiv.org/abs/nucl-ex/0605029).



- 880 [109] F. Hagelstein, R. Miskimen and V. Pascalutsa, *Nucleon Polarizabilities: from*  
881 *Compton Scattering to Hydrogen Atom*, Prog. Part. Nucl. Phys. **88**, 29 (2016),  
882 doi:[10.1016/j.ppnp.2015.12.001](https://doi.org/10.1016/j.ppnp.2015.12.001), [1512.03765](https://arxiv.org/abs/1512.03765).
- 883 [110] R. D. Peccei and H. R. Quinn, *CP Conservation in the Presence of Instantons*, Phys. Rev.  
884 Lett. **38**, 1440 (1977), doi:[10.1103/PhysRevLett.38.1440](https://doi.org/10.1103/PhysRevLett.38.1440).
- 885 [111] R. D. Peccei and H. R. Quinn, *Constraints Imposed by CP Conservation in the Presence of*  
886 *Instantons*, Phys. Rev. D **16**, 1791 (1977), doi:[10.1103/PhysRevD.16.1791](https://doi.org/10.1103/PhysRevD.16.1791).
- 887 [112] F. Wilczek and A. Zee, *Instantons and Spin Forces Between Massive Quarks*, Phys. Rev.  
888 Lett. **40**, 83 (1978), doi:[10.1103/PhysRevLett.40.83](https://doi.org/10.1103/PhysRevLett.40.83).
- 889 [113] S. Weinberg, *A New Light Boson?*, Phys. Rev. Lett. **40**, 223 (1978),  
890 doi:[10.1103/PhysRevLett.40.223](https://doi.org/10.1103/PhysRevLett.40.223).
- 891 [114] B. Ananthanarayan, G. Colangelo, J. Gasser and H. Leutwyler, *Roy equation analysis of*  
892  *$\pi\pi$  scattering*, Phys. Rept. **353**, 207 (2001), doi:[10.1016/S0370-1573\(01\)00009-6](https://doi.org/10.1016/S0370-1573(01)00009-6),  
893 [hep-ph/0005297](https://arxiv.org/abs/hep-ph/0005297).
- 894 [115] I. Caprini, G. Colangelo and H. Leutwyler, *Regge analysis of the  $\pi\pi$  scattering amplitude*,  
895 Eur. Phys. J. C **72**, 1860 (2012), doi:[10.1140/epjc/s10052-012-1860-1](https://doi.org/10.1140/epjc/s10052-012-1860-1), [1111.7160](https://arxiv.org/abs/1111.7160).
- 896 [116] R. Garcia-Martin, R. Kaminski, J. R. Pelaez, J. Ruiz de Elvira and F. J. Yndurain, *The Pion-*  
897 *pion scattering amplitude. IV: Improved analysis with once subtracted Roy-like equations*  
898 *up to 1100 MeV*, Phys. Rev. D **83**, 074004 (2011), doi:[10.1103/PhysRevD.83.074004](https://doi.org/10.1103/PhysRevD.83.074004),  
899 [1102.2183](https://arxiv.org/abs/1102.2183).
- 900 [117] J. Gasser, V. E. Lyubovitskij and A. Rusetsky, *Hadronic atoms in QCD + QED*, Phys. Rept.  
901 **456**, 167 (2008), doi:[10.1016/j.physrep.2007.09.006](https://doi.org/10.1016/j.physrep.2007.09.006), [0711.3522](https://arxiv.org/abs/0711.3522).
- 902 [118] M. Hoferichter, J. Ruiz de Elvira, B. Kubis and U.-G. Meißner, *Roy–Steiner-*  
903 *equation analysis of pion–nucleon scattering*, Phys. Rept. **625**, 1 (2016),  
904 doi:[10.1016/j.physrep.2016.02.002](https://doi.org/10.1016/j.physrep.2016.02.002), [1510.06039](https://arxiv.org/abs/1510.06039).
- 905 [119] T. Das, G. S. Guralnik, V. S. Mathur, F. E. Low and J. E. Young, *Electromagnetic mass*  
906 *difference of pions*, Phys. Rev. Lett. **18**, 759 (1967), doi:[10.1103/PhysRevLett.18.759](https://doi.org/10.1103/PhysRevLett.18.759).
- 907 [120] J. F. Donoghue and A. F. Perez, *The Electromagnetic mass differences of pions and kaons*,  
908 Phys. Rev. D **55**, 7075 (1997), doi:[10.1103/PhysRevD.55.7075](https://doi.org/10.1103/PhysRevD.55.7075), [hep-ph/9611331](https://arxiv.org/abs/hep-ph/9611331).
- 909 [121] B. Ananthanarayan and B. Moussallam, *Electromagnetic corrections in the anomaly sec-*  
910 *tor*, JHEP **05**, 052 (2002), doi:[10.1088/1126-6708/2002/05/052](https://doi.org/10.1088/1126-6708/2002/05/052), [hep-ph/0205232](https://arxiv.org/abs/hep-ph/0205232).
- 911 [122] K. Kampf and B. Moussallam, *Chiral expansions of the  $\pi^0$  lifetime*, Phys. Rev. D **79**,  
912 076005 (2009), doi:[10.1103/PhysRevD.79.076005](https://doi.org/10.1103/PhysRevD.79.076005), [0901.4688](https://arxiv.org/abs/0901.4688).
- 913 [123] P. Masjuan and P. Sanchez-Puertas, *Pseudoscalar-pole contribution to the  $(g_\mu-2)$ : a ratio-*  
914 *nal approach*, Phys. Rev. D **95**(5), 054026 (2017), doi:[10.1103/PhysRevD.95.054026](https://doi.org/10.1103/PhysRevD.95.054026),  
915 [1701.05829](https://arxiv.org/abs/1701.05829).
- 916 [124] M. Hoferichter, B.-L. Hoid, B. Kubis, S. Leupold and S. P. Schneider, *Dispersion*  
917 *relation for hadronic light-by-light scattering: pion pole*, JHEP **10**, 141 (2018),  
918 doi:[10.1007/JHEP10\(2018\)141](https://doi.org/10.1007/JHEP10(2018)141), [1808.04823](https://arxiv.org/abs/1808.04823).

- 919 [125] A. Gérardin, H. B. Meyer and A. Nyffeler, *Lattice calculation of the pion transition*  
920 *form factor with  $N_f = 2 + 1$  Wilson quarks*, Phys. Rev. D **100**(3), 034520 (2019),  
921 doi:[10.1103/PhysRevD.100.034520](https://doi.org/10.1103/PhysRevD.100.034520), [1903.09471](https://arxiv.org/abs/1903.09471).
- 922 [126] D. A. Bryman, P. Depommier and C. Leroy,  *$PI \rightarrow E$  neutrino,  $PI \rightarrow E$  neutrino*  
923 *gamma decays and related processes*, Phys. Rept. **88**, 151 (1982), doi:[10.1016/0370-](https://doi.org/10.1016/0370-1573(82)90162-4)  
924 [1573\(82\)90162-4](https://doi.org/10.1016/0370-1573(82)90162-4).
- 925 [127] V. Cirigliano, M. Knecht, H. Neufeld and H. Pichl, *The Pionic beta decay in chiral per-*  
926 *turbation theory*, Eur. Phys. J. C **27**, 255 (2003), doi:[10.1140/epjc/s2002-01093-2](https://doi.org/10.1140/epjc/s2002-01093-2),  
927 [hep-ph/0209226](https://arxiv.org/abs/hep-ph/0209226).
- 928 [128] V. Cirigliano, S. Gardner and B. Holstein, *Beta Decays and Non-Standard Interactions in*  
929 *the LHC Era*, Prog. Part. Nucl. Phys. **71**, 93 (2013), doi:[10.1016/j.pnpnp.2013.03.005](https://doi.org/10.1016/j.pnpnp.2013.03.005),  
930 [1303.6953](https://arxiv.org/abs/1303.6953).